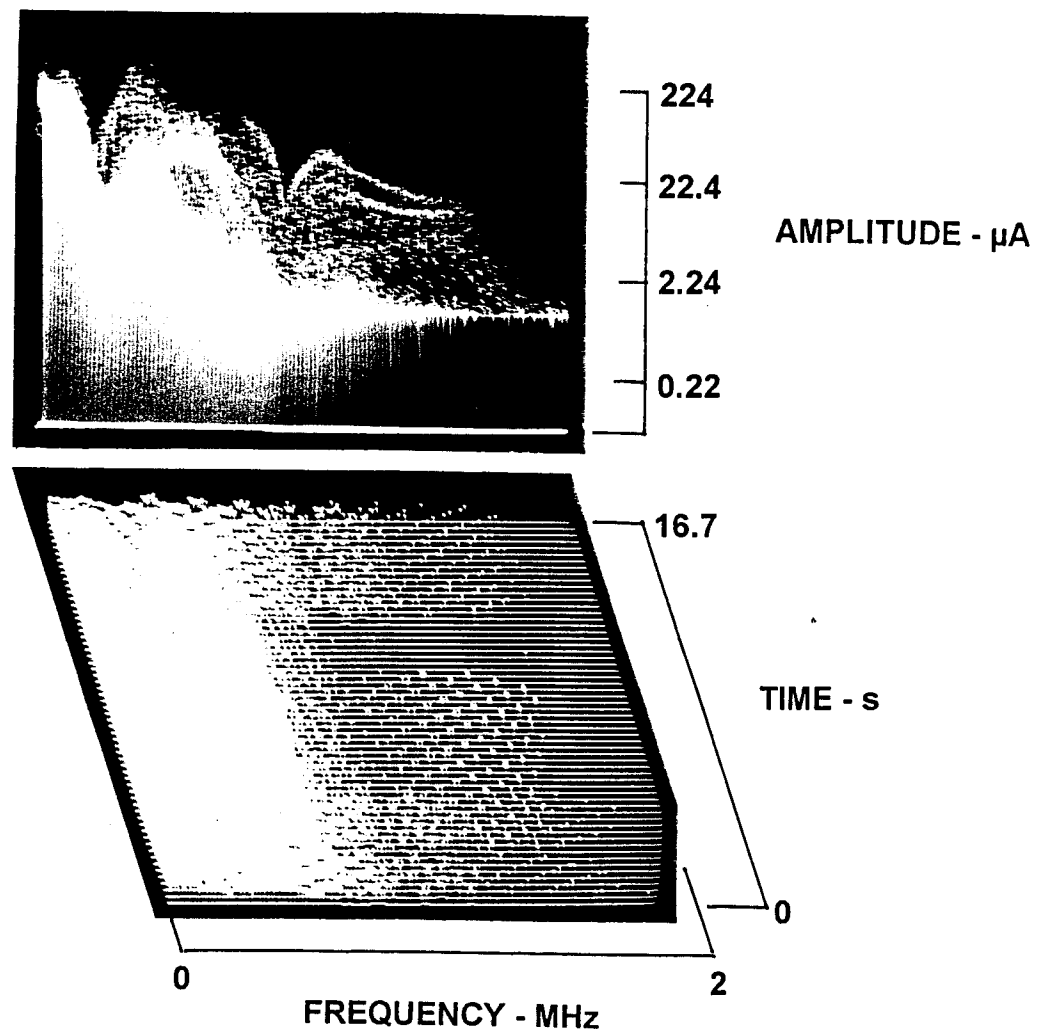


Figure 2.7-2
EMI Current on the Support Wire for a Fluorescent Light Fixture



970501 1427

NW, RFD, Liquatite conduit feeding
fluorescent light, MB

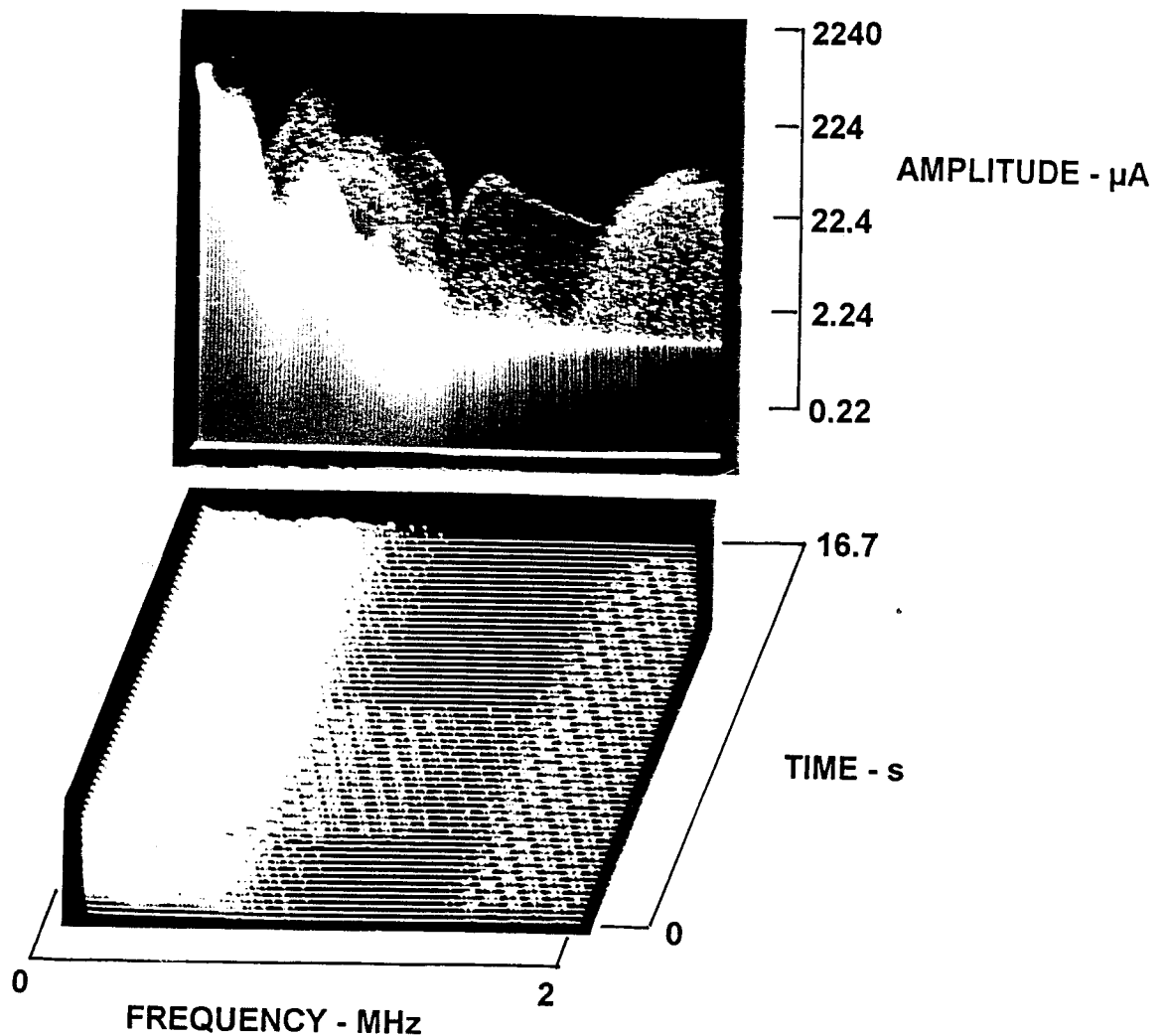
1 MHz, 2 MHz, 30 kHz, 200 ms

F-70, +20, 0, -30

Figure 2.7-3

Time-Varying EMI Current on the Conduit Feeding a Fluorescent Light Fixture,

Example 1



970501 1420

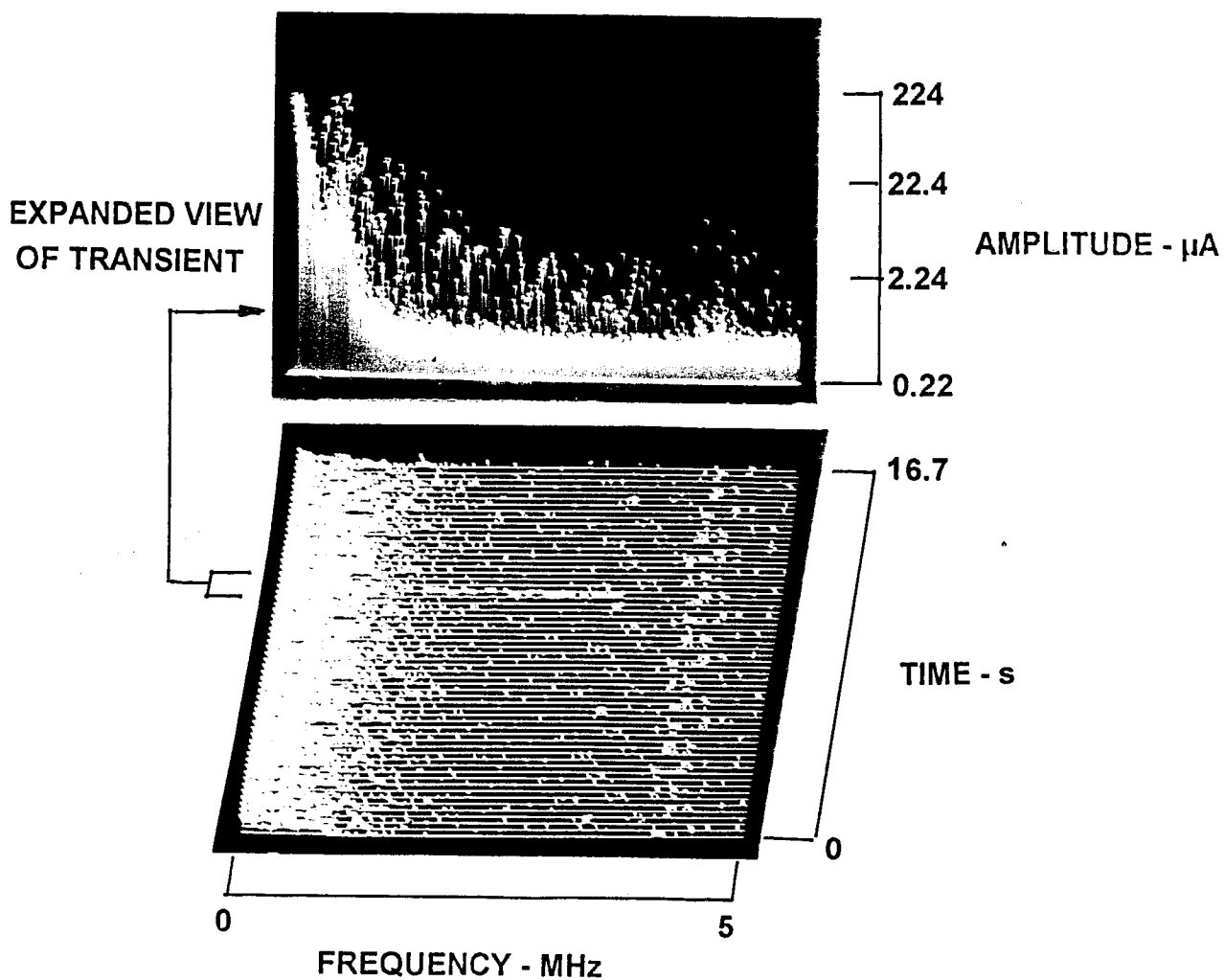
NW, RFD, Liquatite conduit feeding
fluorescent light, MB

1 MHz, 2 MHz, 30 kHz, 200 ms

F-70, +20, 0, -30

Figure 2.7-4

Time-Varying EMI Current on the Conduit Feeding a Fluorescent Light Fixture,
Example 2



970502 1355

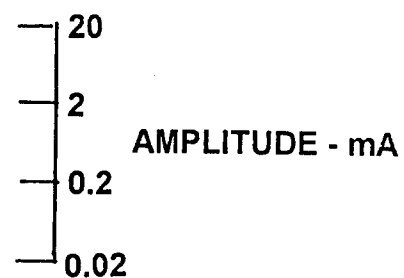
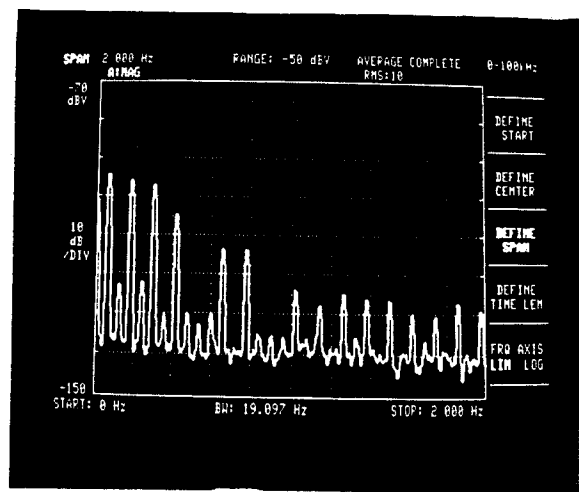
NW, Liqueatite conduit

feeding fluorescent lights, MB

2.5 MHz, 5 MHz, 30 kHz, 50 ms

F-70, +20, 0, -20

Figure 2.7-5
Transient Current on the Conduit Feeding Fluorescent Light Fixture



970502 1108

NW, Liqueatite conduit
feeding fluorescent lights, MB
P6021 (10/1), CT-4 (20/1), 0

Figure 2.7-6
Low-Frequency EMI Current on Conduit Feeding Fluorescent Light Fixture

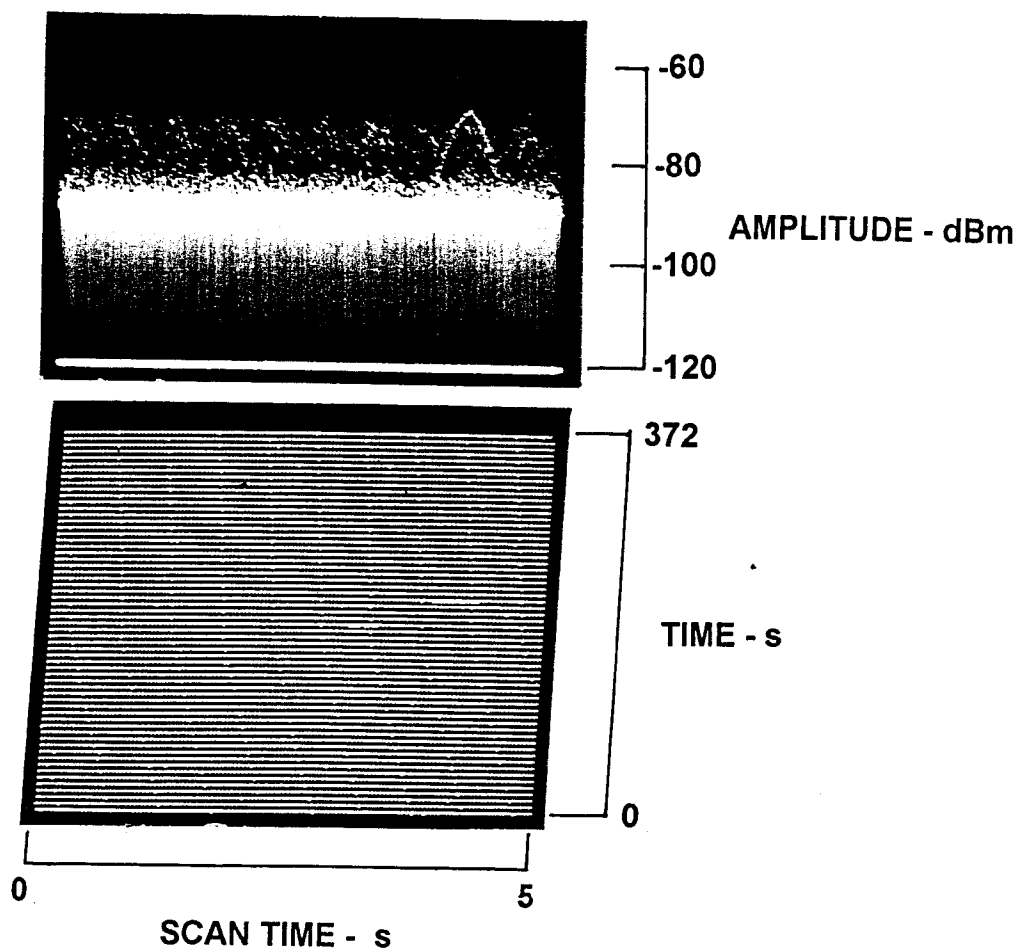
2.8 ELECTRIC FENCE INTERFERENCE

Impulsive radio interference from electric fences was noted throughout the NW9705 survey. While their operation was intermittent, the number causing interference varied from one to as many as four. The period between impulses varied from about one to five seconds. The amplitude of the impulses varied from the operating noise floor up to -70 dBm.

Figure 2.8-1 (970429 0937) shows the temporal structure of interference from a single electric fence. In this example, the impulses were separated about 5.5 seconds apart. The amplitude of each impulse was about -72 dBm.

The wide-band impulses produce annoying pops in the audio output of an HF receiver. They also are sufficiently strong to operate the automatic gain control (AGC) of a receiver. This decreases the gain of the receiver for a short period of time and artificially decreases the amplitude of a received signals until the AGC recovers. The impulses also cause receivers with new-energy alarms to search for a new signal at the occurrence of each impulse. While seemingly a minor interference problem, electric-fence interference can severely degrade the ability of a site to detect and receive radio signals. This is especially true when impulses from multiple fences are received.

Some models of electric-fence controllers do not generate radio interference. The use of these models should be encouraged. Other models generate impulses with very steep wave fronts. Interference from these models can usually be corrected by placing a small capacitor across the terminals of the switch generating the impulses. Since the models of electric-fence controllers frequently change and different models are available in various parts of the country, a specific model cannot be recommended. Those available locally must be examined, and the noise-free models can be recommended to their users.



970429 0937
 NW, RF Rm, LBM 000
 2.8 MHz, 0, 30 kHz, 5 s LS
 BB-1, +20, 0, -20

AT 2.8 MHz

Figure 2.8-1
Interference from an Electric Fence

2.9 COMPARISON OF COMBINED OMNI AND CONICAL MONOPOLE ANTENNAS

Two omni-directional antenna systems are available for signal reception at the Northwest site. The combined omni (CO) of the CDAA is available as well as a Conical Monopole (CM) antenna located south of the CDAA. Since the relative operational merits of the two antennas has never been fully established, an effort was made to compare signal reception from the two antennas. Both antennas were considered to be in good operational condition; however, the coaxial connector at the base of the CM needs to be resealed; it was loose and poorly sealed when examined.

A low-loss coaxial cable from the CM ends under the floor in the RF Room. A power splitter provides two RF signal paths. One splitter output provides signals to SPECOM. The second splitter output supplies signals to a CU1382 multicoupler. Eight multicoupler outputs are available, but no receivers or ENLARGER inputs were connected to the multicoupler at the time of the SNEP team visit.

The NSGA Northwest CO employed only the 120 high-band elements. There is no combiner for the low-band elements. The output of the CO combiner is available for general use. The preamplifier installed at the CO combiner output at some sites was not used at Northwest. Since the dynamic range of the preamplifier commonly employed for this use is inadequate to handle the full dynamic range of the ambient signal population, the present configuration at Northwest is preferred and recommended by the SNEP teams.

The amplitude and noise floor for each test signal from each antenna was measured and compared. The measurements were made at various times of the day and night. Table 2.9-1 provides a summary of signal reception by the two antennas for the high band. The source of the received signal is provided in the first column of the table. If the signal source could not be identified, it was given an S- number. The frequency of each measurement is given in the second column. The operational noise floor (OPR NF) at the time of each measurement is given in Columns 3 and 6 (scaled to the noise floor in dBm for a 3-kHz gaussian-shaped bandwidth). The received signal strength is provided in Columns 4 and 7. The signal/noise (S/N) ratio is provided in Columns 5 and 8. Average values of signal strength and S/N are provided at the bottom row of the table.

Table 2.9-1
COMPARISON OF SIGNAL RECEPTION BY THE CO AND CM ANTENNAS
HIGH BAND

Combined Omni					Conical Monopole		
SOURCE	FREQ MHz	OPR NF dBm	SIGNAL dBm	S/N dB	OPR NF dBm	SIGNAL dBm	S/N dB
LPD	12.65	-115	-102	13	-120	-104	16
S	16.33	-123	-108	14	-121	-106	15
S-1	21.57	-123	-112	11	-120	-108	12
S-2	10.26	-113	-79	34	-125	-87	28
S-3	8.15	-111	-76	35	-104	-50	54
WWV	15	-121	-88	33	-119	-94	25
WWV	20	-118	-110	8	-118	-104	14
			-96.4	21.1		-93.3	23.4

The average strength of all signals for the high band was 3.1-dB higher for the CM than for the CO. The average S/N for all signals was 2.3-dB higher for the CM than the CO. This indicates that the CM is a slightly better collector of high-band signals than the CO, but the advantage is small.

Table 2.9-2 provides the results for the low band. The format of the low-band table is the same as that for the high-band. The average strength of all signals in the low band was 15.9-dB higher for the CM than for the CO, but the average S/N was only 5-dB higher for the CM. This shows that the CM provides significantly higher signal levels than the CO for low-band reception, but external noise sources were received by the CM at higher levels than the CO. Nevertheless, the CM had a signal-reception advantage over the CO. As external noise sources are eliminated, this S/N difference will increase to about the signal-strength difference.

Table 2.9-2

COMPARISON OF SIGNAL RECEPTION BY THE CO AND CM ANTENNAS

LOW-BAND

Combined Omni

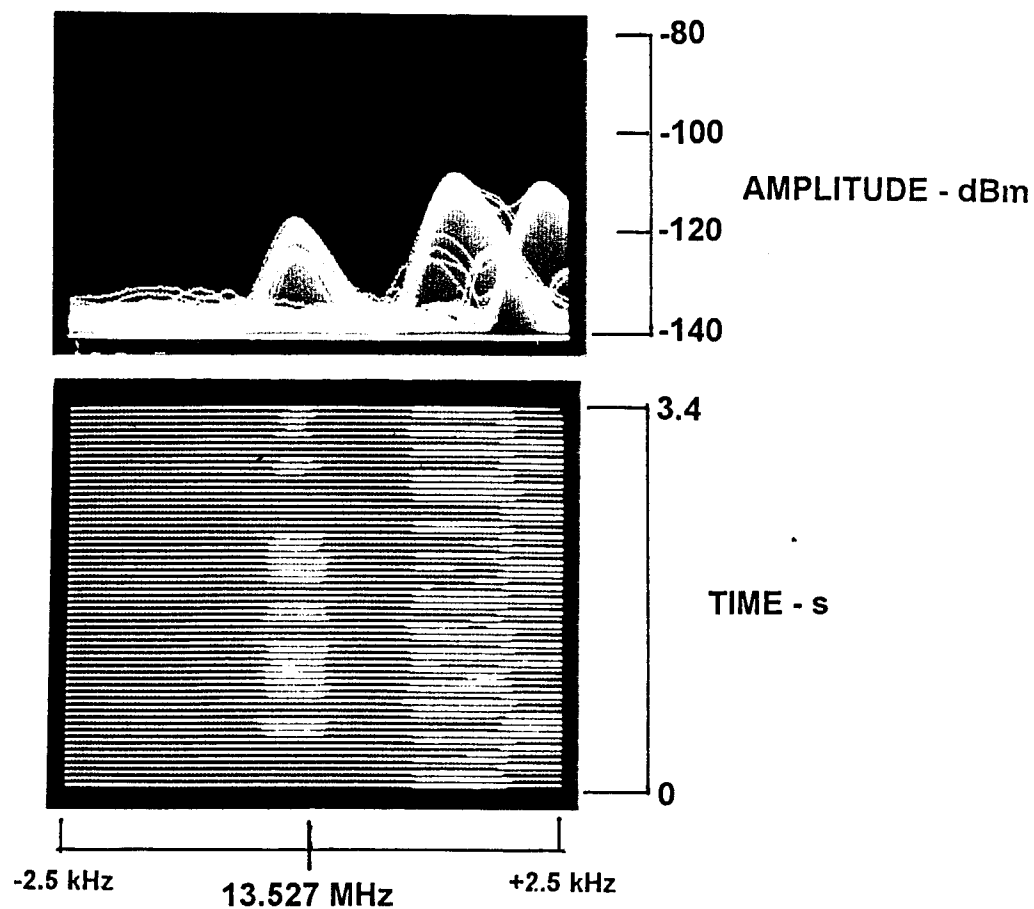
Conical Monopole

SOURCE	FREQ MHz	OPR NF dBm	SIGNAL dBm	S/N dB		OPR NF dBm	SIGNAL dBm	S/N dB
S-4	7.87	-113	-60	53		-109	-56	53
CHU	7.34	-119	-75	43		-107	-64	43
WWV	5	-115	-94	21		99	-74	25
WWV	5	-99	-60	39		-80	-40	40
WWV	5	-101	-60	41		-95	-46	49
WWV	5	-101	-60	41		-87	-43	45
WWV	5	-117	-93	24		-103	-75	28
WWV	5	-116	-102	14		-102	-74	28
WWV	5	-118	-100	18		-103	-74	29
WWV	5	-117	-104	13		-105	-92	13
WWV	2.5	-102	-74	28		-93	-56	37
WWV	2.5	-107	-83	24		-95	-67	28
WWV	2.5	-89	-54	35		-95	-60	35
WWV	2.5	-108	-84	24		-95	-60	35
			-78.8	29.9			-62.9	34.9

2.10 GENERAL SIGNAL RECEPTION

The reception of signals from known sources was examined at intermittent times throughout the survey. Several examples are provided in Section 2.9 where signals received by the Combined Omni (CO) and the Conical Monopole (CM) are compared. These signals, and signals from other sources, were also examined with various CDAA beams. The purpose of this exercise was to obtain some idea of the received signal levels from known sources, and to scale these signal levels to those expected from lower-power sources and sources with less effective antennas. Signal levels obtained in Section 2.9 suggest that the maximum level expected from a 10-kW transmitter using an efficient tuned vertical dipole antenna would be on the order of -70 dBm for a beam pointed directly at the station. This assumes that the source is located within the primary coverage area of the Northwest site. Since a 100-watt transmitter operating with the same antenna would provide a maximum signal level about 20-dB lower in amplitude, or about -90 dBm, the site must be concerned with the reception of low-level signals. Since received signal levels are also dependent on the variable reflectivity of, and absorption from, ionospheric layers, received signals actually vary from a maximum level down to the lowest possible detectable level of a site. This is why a low operating noise floor and low RFD loss are absolutely essential for the successful operation of a CDAA site.

The amplitude of signals from known sources and received on beams pointed in the direction of the sources was also measured. Figure 2.10-1 (970430 1308) shows a signal from a high power HF beacon located in the secondary coverage area of the Northwest site. The amplitude of the signal was -120 dBm. The signal is below the operating noise floor of the site for a standard 3-kHz bandwidth. In order to receive the signal, it was necessary to decrease the signal-detection bandwidth to 100 Hz. If the same source was located in the primary coverage area it would be about 15-dB stronger. Since the transmitter power is more than 10 kW and the transmitting antenna is an efficient tuned monopole, the example demonstrates the need for a low noise floor at the input terminals of a receiver as well as low RFD signal loss.

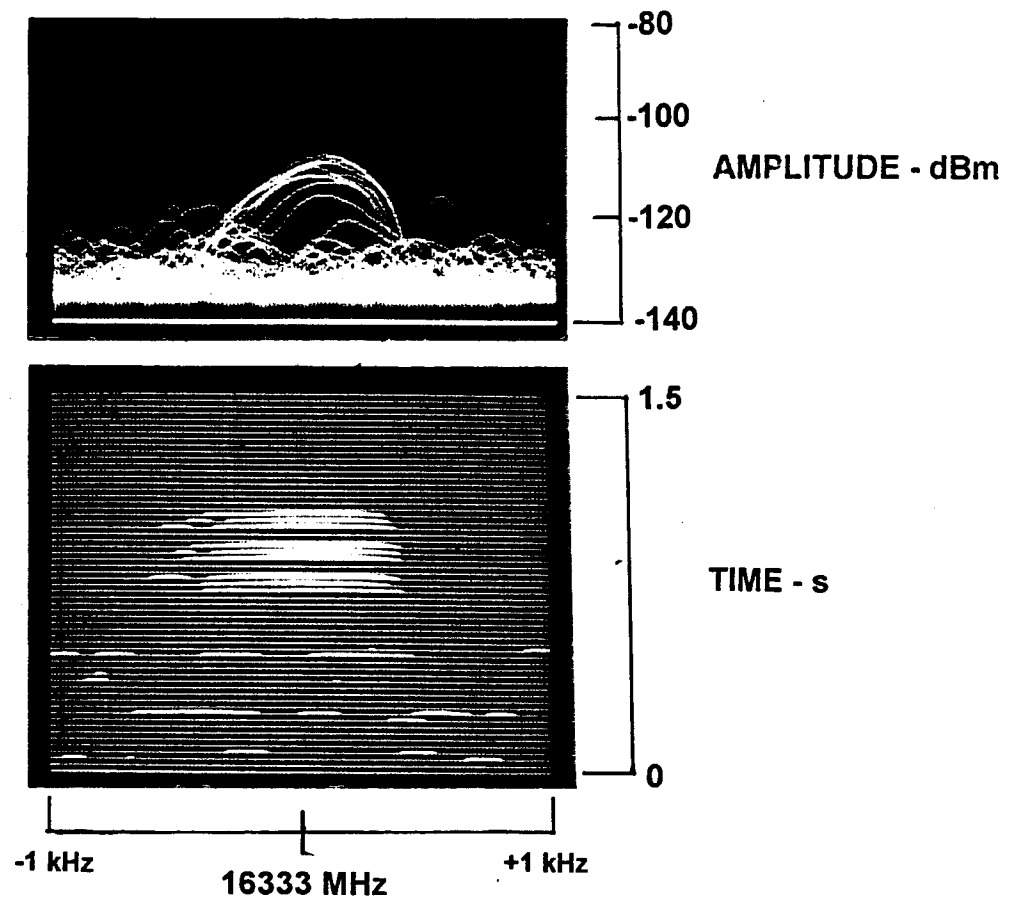


970430 1308
 NW, RFD, HBM 048
 13.527 MHz, 5 kHz, 0.1 kHz, 50 ms
 BPF-4, +20, 0, -40
 C-Beacon

Figure 2.10-1
Beacon Reception, Example 1

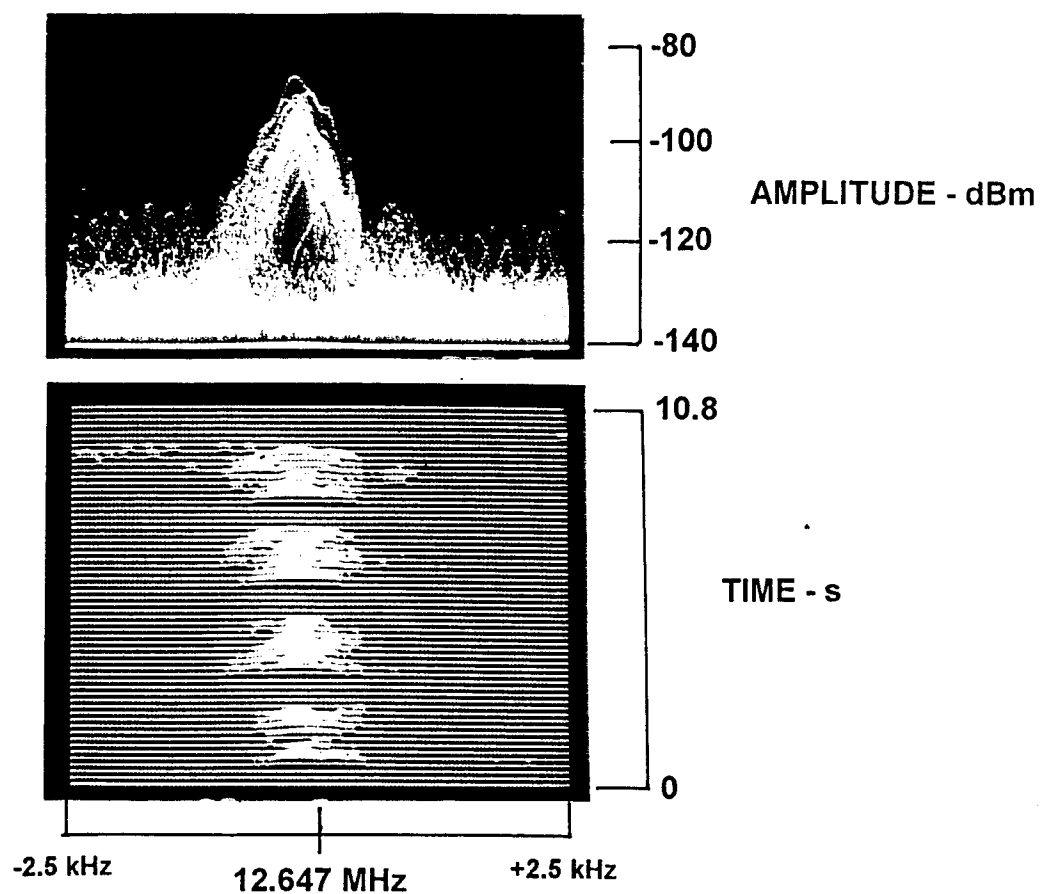
Figure 2.10-2 (970430 1500) shows a signal received from another HF beacon located in the secondary coverage area of the site. It also has a transmitter power in excess of 10 kW and employs an efficient tuned-monopole antenna. The received amplitude was -107 dBm, somewhat higher than the prior example. It was detected with a 300-Hz bandwidth. This signal was barely detectable with the 3-kHz bandwidth of a standard receiver.

A third example of high-power-signal detection is shown in Figure 2.10-3 (970430 1356). The source is Station LPD in Argentina which employs a high power transmitter and an antenna with positive gain. It is also located in the primary coverage area of the site. Because of these factors a stronger received signal level would be expected. The received signal strength was -86 dBm at the time of the measurement. This is above the normal operating noise floor of the site for a 3-kHz bandwidth. However, one must remember that this is an example of the maximum received signal level from LPD. Over time, the received level will vary from this maximum level downward into the operating noise floor of the site. It is estimated that this signal will exceed a level of -95 dBm only 50% of the time. It will be lower than -95 dBm about 50% of the time. Thus, the probability of the intercept of such signals will increase dramatically as the operating noise floor and RFD loss are decreased.



970430 1500
 NW, RFD, Con Monopole
 16.333 MHz, 2 kHz, 0.3 kHz, 50 ms
 +20, 0, -40
 S-Beacon

Figure 2.10-2
Beacon Reception, Example 2



970430 1356
 NW, RFD, HBM 168
 12.647 MHz, 5 kHz, 0.3 kHz, 100 ms
 +20, 0, -40
 LPD Argentina

Figure 2.10-3
Beacon Reception, Example 3

3. SIGNAL RECEPTION EVALUATION

3.1 APPROACH

The impact of site parameters and harmful levels of EMI on the ability of the Northwest CDAA site to receive typical kinds of radio signals was investigated. The Performance Evaluation Technique (PET-2)⁵ developed by the Naval Postgraduate School was used to establish numerical values describing the impact of site parameters and EMI on signal reception. The evaluation requires that specific signal sources be selected and measured site parameters be used. Table 3-1 lists the sources along with the primary operating parameters of each source.

Table 3-1
Signal Sources

Source No.	Source Zone	Beam Degrees	Lat.	Lon.	Power W	Antenna Type	Modulation	Detection Threshold
1	Secondary	84	23.5 N	18.5 W	100	Whip	Digital	12 dB
1A	Primary	84	34 N	45 W	100	Whip	Digital	12 dB
2	Primary	156	15 N	67 W	100	Whip	Digital	12 dB
2A	Primary	156	15 N	67 W	5,000	CM	Digital	12 dB

Sources 1, 1A, and 2 in Table 3-1 are typical parameters for HF communications transmitters on medium-size motor vessels. Source 2A is provided for comparative purposes. The locations are on sea lanes used by such vessels. Source 1 is located in the secondary coverage zone of Beam 084 of the Northwest site; the transmitter power is 100 watts. A 16-ft whip antenna is employed, and digital modulation is used with a threshold detection level of 12 dB.

Source 1A is identical to Source 1, is also located in Beam 084, and is in the primary coverage area of the Northwest site. Source 2 is identical to Source 1 except that it is located in the primary coverage area for Beam 156. Source 2A is the same as Source 2 except that the transmitter power is increased from 100 watts to 5,000 watts, and the antenna is changed to a conical monopole.

⁵ Wilbur R. Vincent and Richard W. Adler, *A Method of Evaluating the Ability of Naval Receiving Sites to Detect and Process data from Signals of Interest*, Technical Memorandum PET9608, August 1996.

Monthly average signal amplitudes at the output of the Northwest site's beamformers for Beams 084, 156, and 252 were determined for each hour of the day for each in-beam source by the PROPHET HF propagation-prediction program. Any predicted signal with a $(S+N)/N$ ratio higher than a selected modulation-detection threshold (0 and 12 dB for the examples chosen) was considered detectable. Degradation in signal reception caused by RFD attenuation, RFD noise, and EMI was determined from measured site parameters.

For convenience, a map showing the location of each source is provided. This map also provides the distance from the source to the site in kilometers and the bearing from the site to the source. Since the map is not a great-circle type, the propagation path and the azimuth angles are not properly shown. The source can be located on the great circle map provided in Section 2.1, and the propagation path from each source to the site will be a straight line on that projection.

In addition, the output of the PROPHET field strength (FS) module for each propagation path is provided for reference. This output is provided for the month of the NW9705 survey. Similar outputs can be provided for any month of any year. The portion of PROPHET used to determine received signal parameters provides monthly average values for the maximum useful frequency (MUF) and the lowest usable frequency (LUF). Since these values change with solar illumination of the ionosphere, diurnal variations of MUF and LUF are shown. Hourly values of signal strength, in increments of 2 MHz across the propagating range of frequencies, are provided by the FS module. The signal strength is voltage in $\text{dB}\mu\text{V}$ at the output terminals of a beamformer. Because of the method used to approximate the antenna pattern of a beam of an AN/FRD-10 antenna, it is necessary to add 8 dB to the output of the PROPHET FS module. For computational convenience, this is accomplished at a later stage in the PET-2 program in this document.

Some knowledge of the propagation of HF signals is required to fully interpret the predicted results. A review of the PROPHET manual⁶ and a recently published document on HF propagation is suggested.⁷

⁶ R. B. Rose, *Advanced Prophet HF Assessment System, Users Guide*, Technical Document 692, Naval Ocean Systems Center, San Diego, CA 92152.

⁷ George Jacobs, Theodore J. Cohen, and Robert B. Rose, *The New Shortwave Propagation Handbook*, CQ Communications, 1995.

3.2 RECEPTION OF SOURCE 1

Figure 3.2-1 shows the location of Source 1. The source is located off the coast of northwestern Africa at a distance of 5,630 km from the Northwest site. The source is in the secondary coverage area of the Northwest site; thus, signals from Source 1 will be about 15-dB lower in amplitude than signals from an equivalent source located in the primary coverage area. Also, the propagating frequency range will be lower and more variable than for the same source in the primary coverage area.

Table 3.2-1 shows the predicted values of signal strength in dB μ V for Source 1 at the beamformer output terminals. Data in this table is the primary signal amplitude input to the PET-2 signal reception evaluation program. It assumes there is no signal loss between the antenna elements and the beamformer output.

PET-2 reformats the PROPHET data into decibels above the noise floor of the primary multicouplers. The average value of the noise floor of the primary multicouplers feeding the beamformer is normally found to be about -130 dBm in a 3-kHz gaussian-shaped bandwidth. Any signal intercepted by the antenna elements forming the beam pointed toward Source 1, and exceeding the noise floor, is shown. The noise floor will change with the bandwidth used to detect a signal. Since 3-kHz is a typical signal-detection bandwidth for many receiving systems, it is used in this analysis. Other values of bandwidth and their equivalent noise floor can be used for special cases.

The PET-2 program shows how many signals exceed the noise floor and by how much they exceed the noise floor. Figure 3.2-2 summarizes the site's inherent ability to receive signals from Source 1. Of interest is that this view also shows when and what frequencies can be received from Source 1 by a Morse-code operator, assuming that he can detect and copy a Morse signal at a (S+N)/N of 0 dB. The data show that the site has the inherent capability to receive Morse signals during nighttime hours over a limited frequency range. Daytime signal reception is not feasible. Since the reason for the loss of daytime signal reception is due to lack of support from the reflecting layers of the ionosphere, no site modification or site improvement will provide reliable daytime reception.

Figure 3.3-2A provides the same data as the previous figure with the amplitude highly compressed.

Distance = 5,630 kilometers Bearing = 87.8 degrees

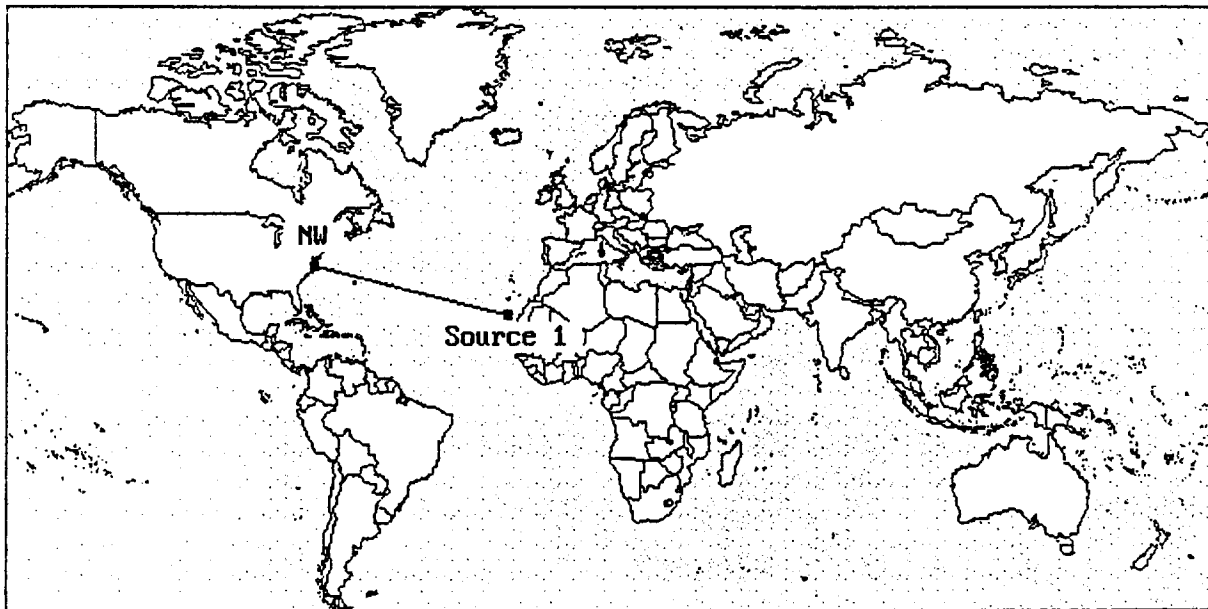


Figure 3.2-1
Map Showing Location for Source 1

Table 3.2-1
PROPHET Output for Source 1

*** UNCLASSIFIED ***

DATE: 5/15/97 ATMOSPHERIC NOISE: NO
10.7 CM FLUX: 73.0 X-RAY FLUX: .0010 MAN-MADE NOISE: QM
SITE1 LAT: 23.5 W LON: 18.5 ANT: 111 @ *OMNI* PWR: 100.00
NW LAT: 36.5 W LON: 76.3 ANT: 115 @ *OMNI* RANGE: 5661 KM

SIGNAL STRENGTH (DB ABOVE 1 MICROVOLT)

	FREQUENCY						
TIME 2	8	16	24	32	40	LF	MF
00	-17-14-13-11-10					2	16
01	-17-14-13-11-10					2	16
02	-17-14-13-11					2	15
03	-17-14-13-11					2	15
04	-17-14-13-15					2	14
05	-17-14-13					2	12
06	-17-14					2	11
07	-17-14					2	12
08	-18-16					3	12
09						5	14
10						6	15
11						8	17

FS>

*** UNCLASSIFIED ***

DATE: 5/15/97 ATMOSPHERIC NOISE: NO
10.7 CM FLUX: 73.0 X-RAY FLUX: .0010 MAN-MADE NOISE: QM
SITE1 LAT: 23.5 W LON: 18.5 ANT: 111 @ *OMNI* PWR: 100.00
NW LAT: 36.5 W LON: 76.3 ANT: 115 @ *OMNI* RANGE: 5661 KM

SIGNAL STRENGTH (DB ABOVE 1 MICROVOLT)

	FREQUENCY						
TIME 2	8	16	24	32	40	LF	MF
12						8	18
13						9	18
14						9	19
15						9	20
16						9	20
17						9	20
18						8	20
19	-19					7	20
20	-18-15					6	19
21	-17-14-12					5	19
22	-18-16-13-11-10					3	18
23	-18-15-13-11-10 -9					2	19

FS>

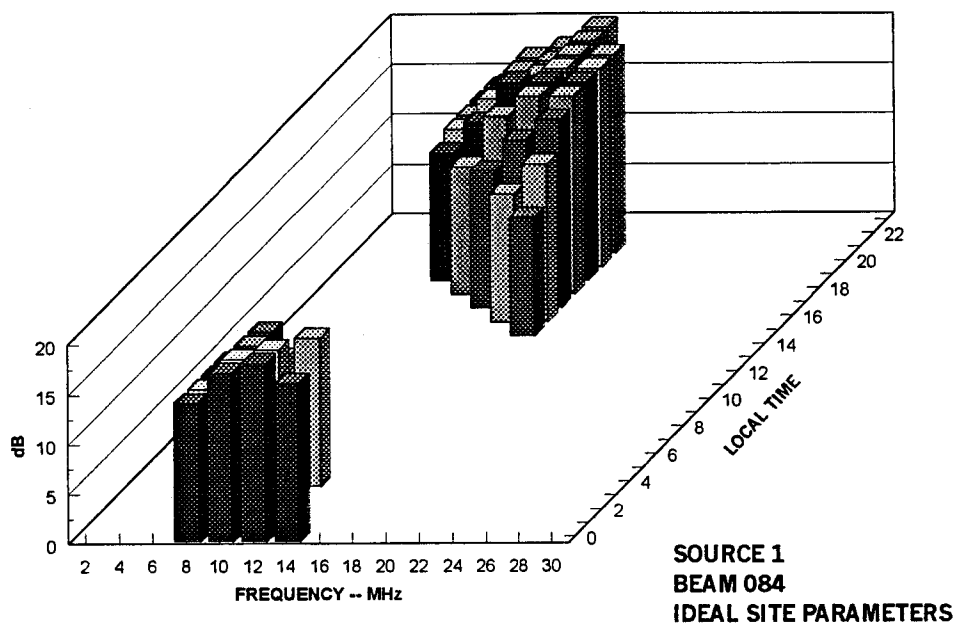


Figure 3.2-2

Signals from Source 1 Exceeding Noise Floor of Primary Multicouplers

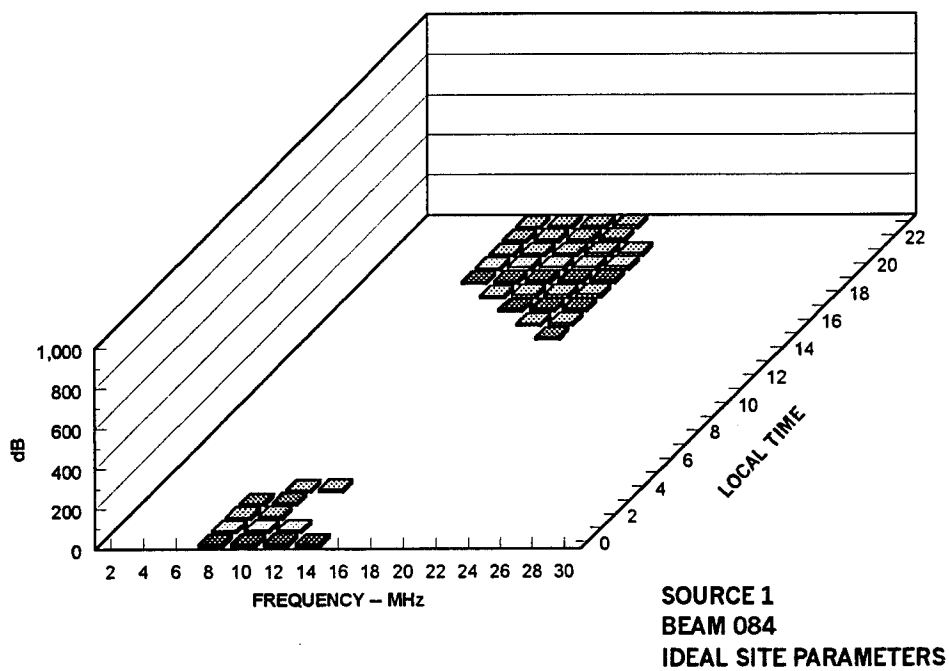


Figure 3.2-2A

Compressed View of Data in Figure 3.2-2

The number of time-frequency bins providing usable signals at the Northwest site can be counted in Figure 3.2-2A. Forty-six time-frequency bins, on the average, were available for the reception of signals. Occasionally signals will be received at times other than shown, and some signals will be received above and below the frequency range shown. This is because the reflection layers of the ionosphere are variable and change with time. Also, the propagating range varies with season, solar activity, and geographic location. Thus, PROPHET must be rerun for any specific time of special interest.

Figures 3.2-2 and 3.2-2A depict the ability of the site to receive manual Morse-code signals from Source 1. Machine-detected signals require a positive signal-to-noise margin, and many types of automatic-detected signals require a detection margin of +12 dB. This additional margin will exclude some low-level signals from detection. The extent of this loss was explored by PET-2. Figures 3.2-3 and 3.2-3A show the impact of the signal-detection margin on the reception of signals from Source 1. A total of 45 time-frequency bins exceeded the required threshold. Only one time-frequency bin was lost, representing a small loss of about 4 percent.

The amplitude of some signals intercepted by the antenna is reduced by signal loss in the RFD. In addition, some signals are covered by RFD-generated noise. The impact of these two site factors is examined by PET-2. Figure 3.2-4 shows the number of time-frequency bins that exceed the combined effect of the signal-detection margin, RFD loss and RFD noise. Eleven time-frequency bins exceeded combined effects of the three factors. Thirty-four time-frequency bins were lost, a loss in signal-detection capability of 74%.

Next, the impact of external and internal noise, called the operating noise floor, was added to the signal-detection process. Hourly values of the operating noise floor for Beam 084 are provided in Table 2.2.3-1. These values were used in the evaluation, and Figure 3.2-5 shows the result. No signals exceeded the combined impact of detection threshold, RFD loss, RFD noise, and the operating noise floor. This represents the ability of the site to receive machine-detected signals from Source 1 at the time of the survey. In evaluating this result, it must be remembered that the power of the source is relatively low (100 W), the antenna is typical field deployable vehicular antenna (16-ft. whip), and the source is located in the secondary coverage area of the receiving site. Higher power, a better transmitting antenna, and moving the source into the primary coverage area will increase signal detectability.

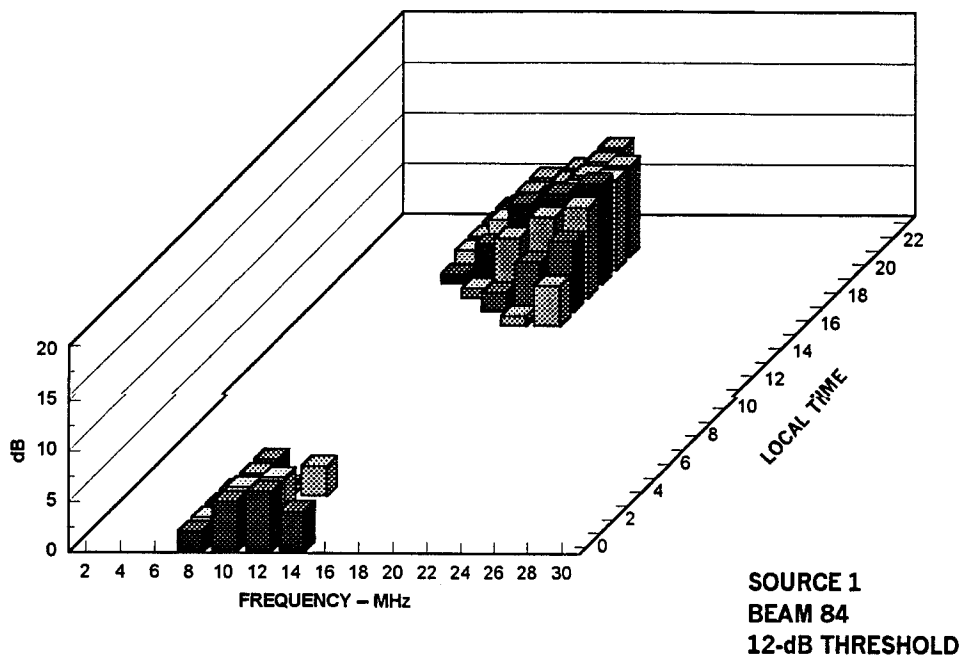


Figure 3.2-3

Signals from Source 1 Exceeding the Noise Floor of the Multicouplers and
a 12-dB Detection Margin

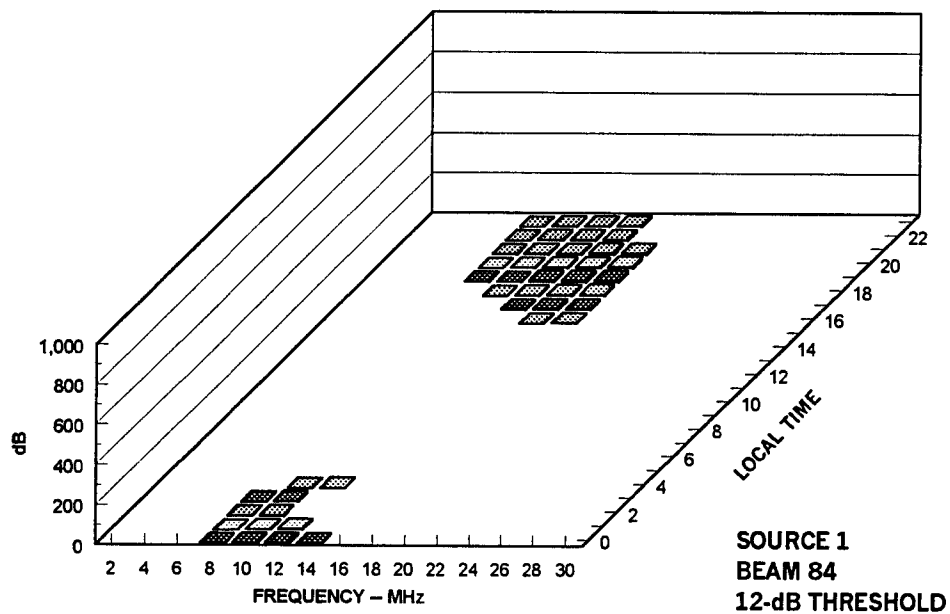


Figure 3.2-3A

Compressed View of Data in Figure 3.2-3

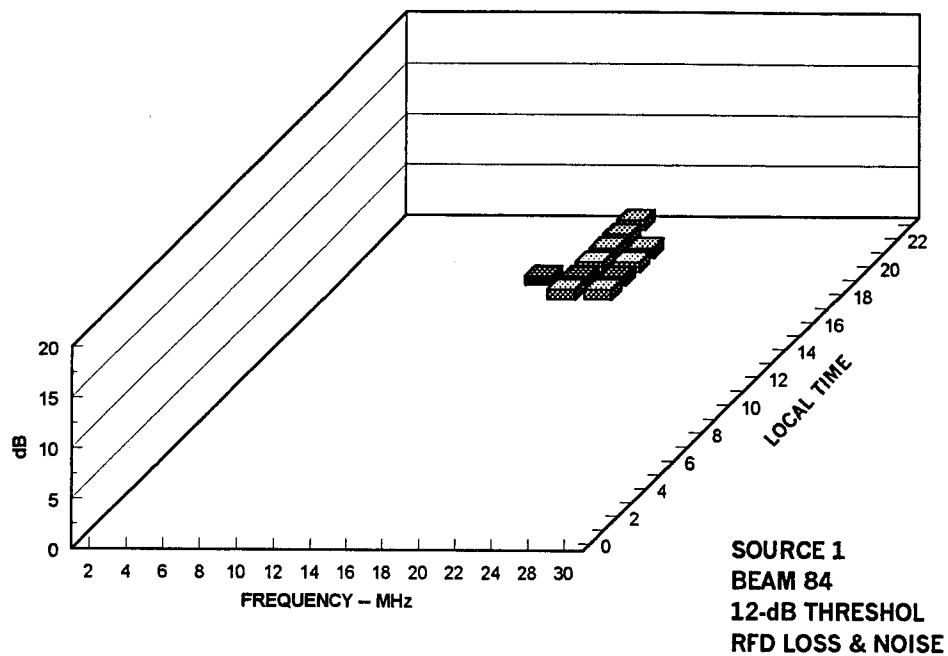


Figure 3.2-4

Signals from Source 1 Exceeding the Detection Margin, RFD Loss, and RFD Noise

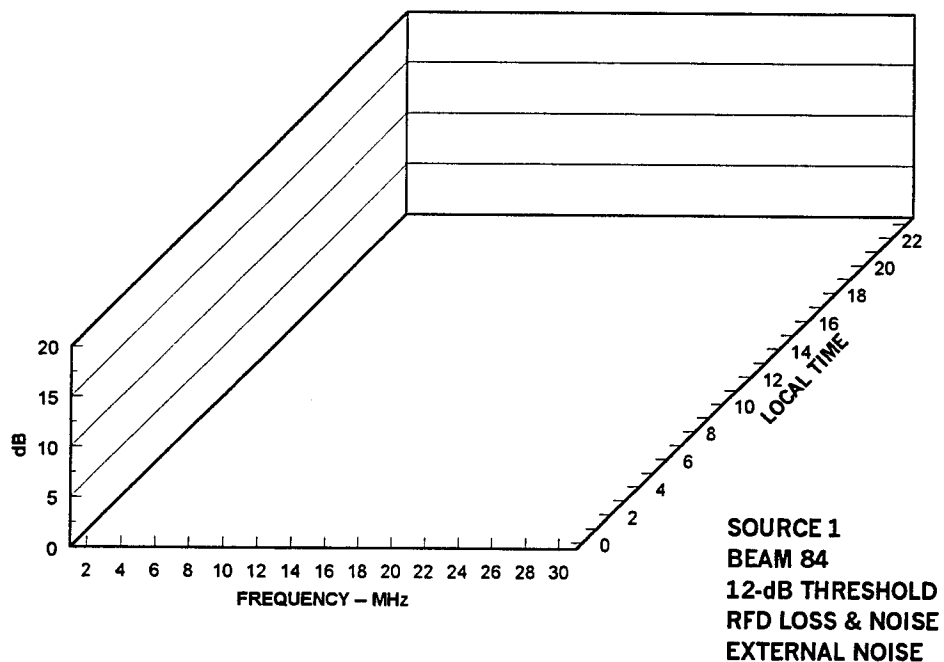


Figure 3.2-5

Signals Exceeding the Detection Margin, RFD Loss, and the Operating Noise Floor

3.3 RECEPTION OF SOURCE 1A

Source 1 was moved from its location in the secondary coverage area to a new location in the primary coverage area. It was then identified as Source 1A. The new location is in the central part of the Atlantic Ocean, and it remains within Beam 084. Figure 3.3-1 shows the new location. It is 2,857 kilometers from the Northwest site and provides a more favorable single-hop propagation path from the source to the receiving site.

Table 3.3-1 provides the PROPHET predictions of the MUF, LUF, and signal strength in dB μ V at the output terminals of the beamformer. Again, 8 dB is added to these values in the PET-2 program to account for the beam gain of the receiving antenna. The values of signal amplitude at the output of the beamformer are considerably higher than for Source 1 because of the improved propagation path employed for Source 1A.

The PET-2 program reformatted the PROPHET data into decibels above the noise floor of the primary multicouplers. Again, a noise floor value of -130 dBm in a 3-kHz gaussian-shaped bandwidth is used. This assumes that signal reception will be based on a 3-kHz receiving-system bandwidth, a typical detection bandwidth for many receiving systems. Figure 3.3-2 shows a plot of the frequency range and amplitude of signals from Source 1A. Figure 3.3-2A shows a compressed view of the same data. The data from Source 1A can be compared to the equivalent information from Source 1 (see Figures 3.2-2 and 3.2-2A). The frequency range of the received signals is wider and the amplitudes are higher than from the same source when located in the secondary coverage area. The data in Figure 3.3-2 represent optimum signal-reception conditions at the Northwest site since site factors that degrade reception have not yet been included. The data also represents the signal-reception capability for Morse code signals by an experienced operator. This is about the capability of the site when it was first placed into operation.

The highly compressed view in Figure 3.3-2A provides a means to count the time-frequency bins that produce usable signals. A total of 127 time-frequency bins provide signals exceeding the noise floor of the primary multicouplers. This can be compared to a total number of bins of 46 when the same source was located in the secondary coverage area.

Distance = 2,857 kilometers Bearing = 86.9 degrees

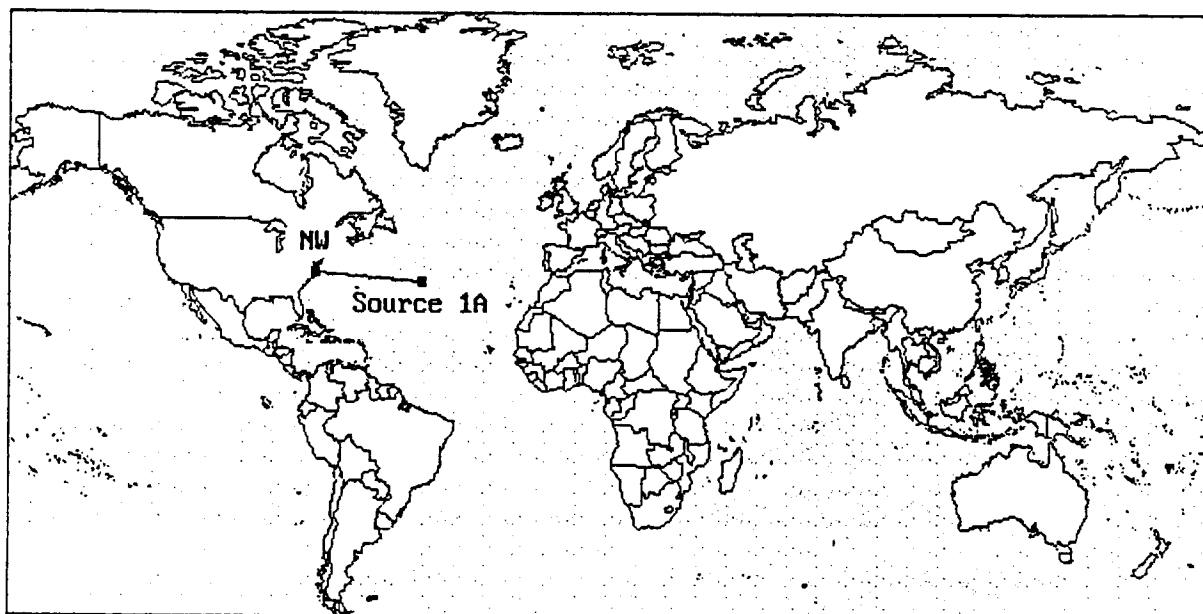


Figure 3.3-1
Map Showing Location of Source 1A

Table 3.3-1

PROPHET Output for Source 1A

*** UNCLASSIFIED ***

DATE: 5/15/97 ATMOSPHERIC NOISE: NO
 10.7 CM FLUX: 73.0 X-RAY FLUX: .0010 MAN-MADE NOISE: QM
 SITE1A LAT: 34.0 W LON: 45.0 ANT: 111 @ *OMNI* PWR: 100.00
 NW LAT: 36.5 W LON: 76.3 ANT: 115 @ *OMNI* RANGE: 2839 KM

SIGNAL STRENGTH (DB ABOVE 1 MICROVOLT)

TIME	FREQUENCY								LF	MF	
	2	8	16	24	32	40	LF	MF			
00	-18-11	-8	-6	-4	-2	-1	0			2	18
01	-18-11	-8	-6	-4	-2	-1	-4			2	18
02	-18-11	-8	-6	-4	-2	-1				2	16
03	-18-11	-8	-6	-4	-2	-1				2	16
04	-18-11	-8	-6	-4	-2	-20				2	15
05	-18-11	-8	-6	-4	-2	-19				2	15
06	-18-11	-8	-6	-4	-10					2	14
07	-18-11	-8	-6	-15						2	12
08	-18-11	-8	-6	-4						2	12
09	-18-11	-8	-6	-17						2	13
10	-17-13	-9	-6							3	15
11	-17-13	-8	-6							4	16

FS>

*** UNCLASSIFIED ***

DATE: 5/15/97 ATMOSPHERIC NOISE: NO
 10.7 CM FLUX: 73.0 X-RAY FLUX: .0010 MAN-MADE NOISE: QM
 SITE1A LAT: 34.0 W LON: 45.0 ANT: 111 @ *OMNI* PWR: 100.00
 NW LAT: 36.5 W LON: 76.3 ANT: 115 @ *OMNI* RANGE: 2839 KM

SIGNAL STRENGTH (DB ABOVE 1 MICROVOLT)

TIME	FREQUENCY								LF	MF	
	2	8	16	24	32	40	LF	MF			
12	-20-16-12	-8	-17							5	17
13	-19-14-11	-7								6	18
14	-16-13-10									6	19
15	-17-13-11-17									6	20
16	-17-14-11-12									6	20
17	-17-13-11	-7								6	20
18	-16-13-10	-7								6	20
19	-19-14-11	-7	-6							6	20
20	-20-16-12	-8	-5	-4						5	20
21	-16-13	-8	-6	-4	-8					4	20
22	-17-13	-8	-5	-4	-2	-12				3	19
23	-18-11	-8	-6	-3	-2	-1	-18			2	19

FS>

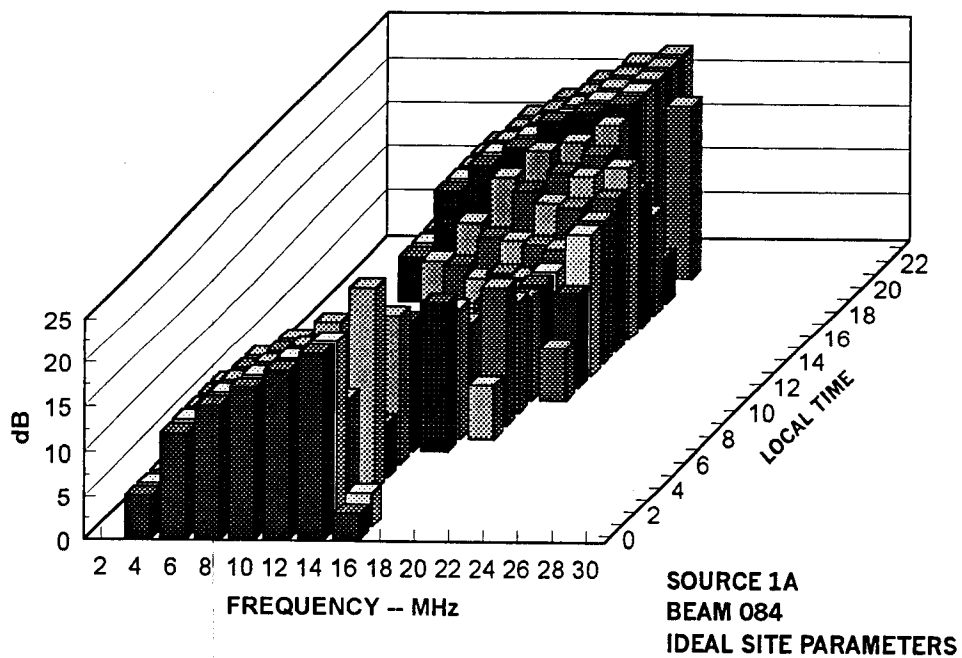


Figure 3.3-2

Signals from Source 1A Exceeding Noise Floor of Primary Multicouplers

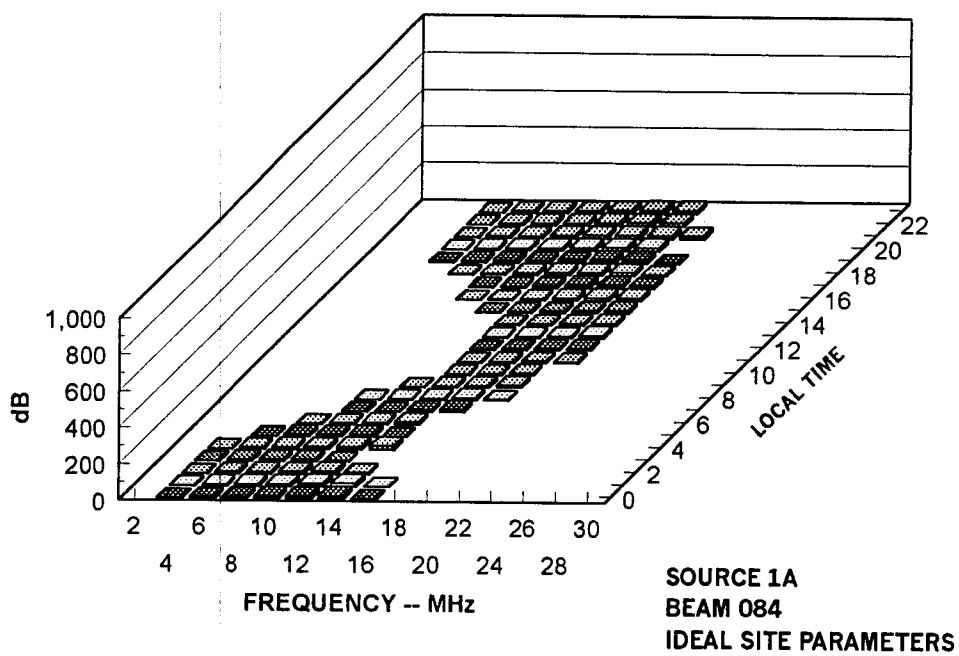


Figure 3.3-2A

Compressed View of Figure 3.3-2

Design changes in the site configuration or antenna configuration are not likely to significantly increase the number of usable time-frequency bins since the AN/FRD-10 antenna at Northwest is already the most efficient signal collector normally available in such sites. A slight increase in the number of time-frequency bins available for signal reception probably will occur in winter months when ionospheric absorption effects are lower at the low-frequency portion of the HF band.

The data in Figures 3.3-2 and 3.3-2A are used as the first reference point for the evaluation of the impact of site parameters and radio noise on the reception of Source 1A. The second step is to examine the impact of the detection margin on the reception of signals from Source 1A. A 12-dB threshold is assumed for the automatic detection of the test signal. Figures 3.3-3 and 3.3-3A show signals that exceed the detection margin. The amplitude scale of the earlier example has been maintained for comparative purposes. A comparison of Figures 3.3-2 with 3.3-3 shows the reduction in signal amplitude above the threshold levels for the two cases. Eighty-eight time-frequency blocks exceed the detection margin. It is clear that the site can receive Morse code signals better than a digital signal which requires a signal-detection margin. This indicates that there is a significant penalty, in this case, to pay for the automatic detection of signals. The number of time-frequency blocks in Figure 3.3-3 exceeding the signal-detection threshold is used as the reference to ascertain the impact of site parameters and man-made radio interference on signal reception.

Figure 3.3-4 shows the impact of measured values of RFD loss and RFD noise on the reception of signals from Source 1A. Thirty-seven time-frequency bins produce usable signals. Fifty-one time-frequency blocks were lost because of RFD loss and the small amount of noise added by components of the RFD, a decrease in signal-reception capability of 58%. This loss can be regained by the elimination of RFD loss and RFD noise.

Of interest is that the existing RFD loss and the added noise at the Northwest site were introduced by site improvements made during and from the installation of automatic beam switching. This is a severe penalty to pay for a site improvement.

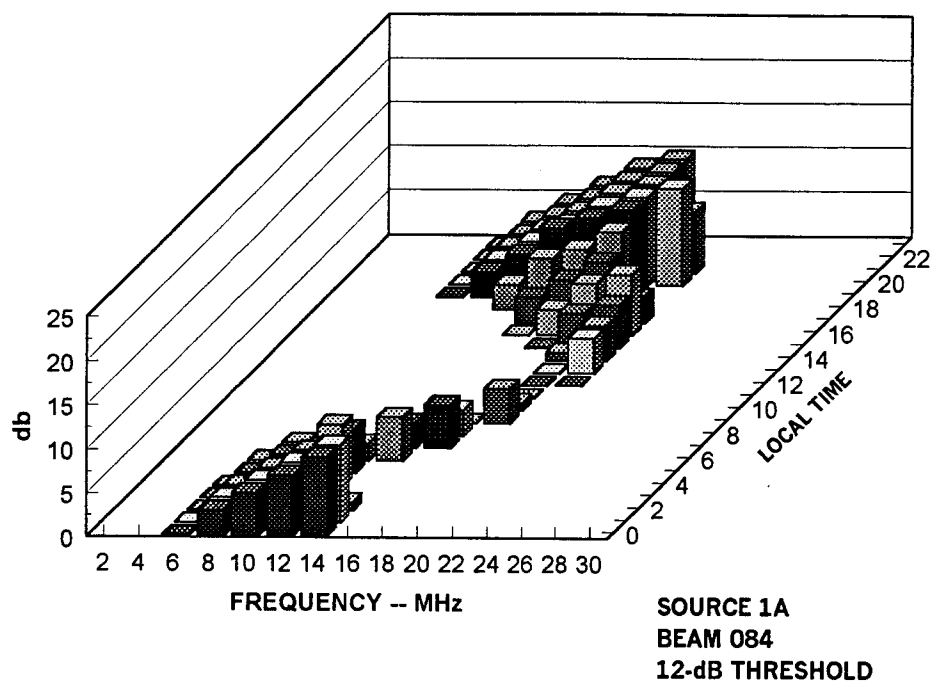


Figure 3.3-3

Signals from Source 1 Exceeding the Noise Floor of the Multicouplers and
a 12-dB Detection Margin

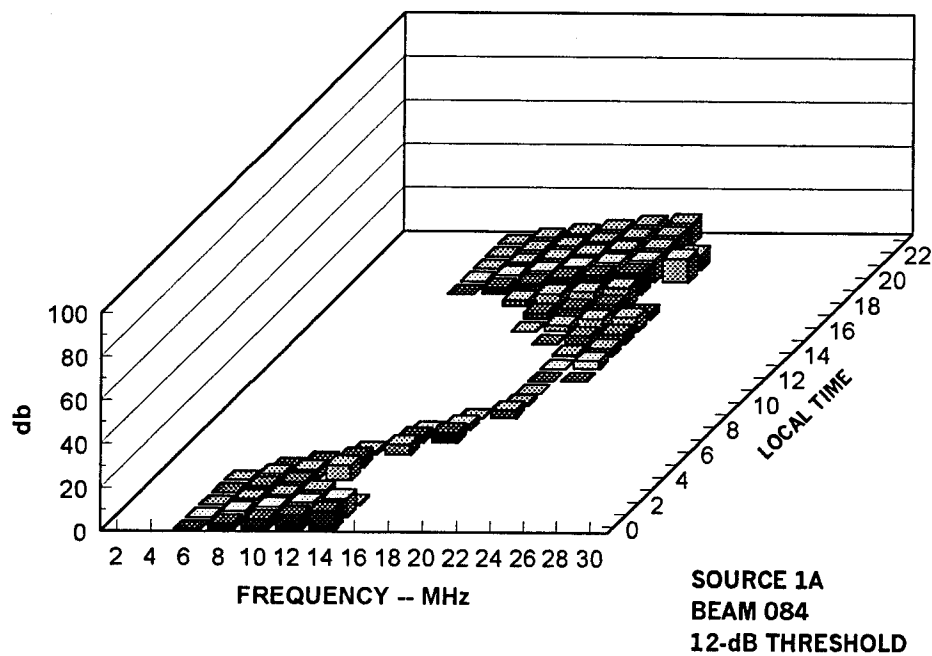


Figure 3.3-3A

Compressed View of Figure 3.3-3

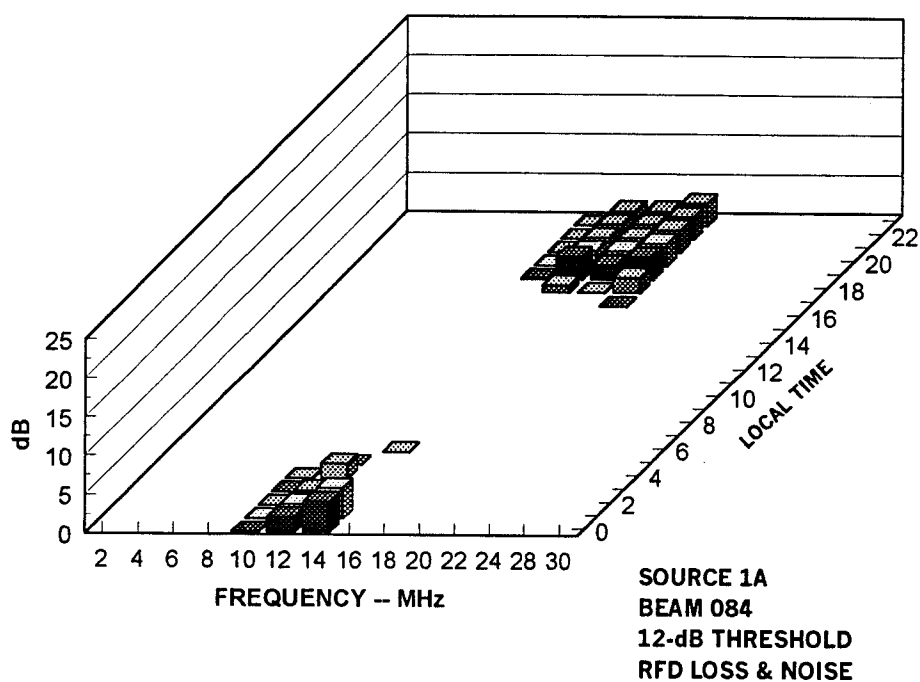


Figure 3.3-4

Signals from Source 1A exceeding Detection Margin, RFD Loss, and RFD Noise

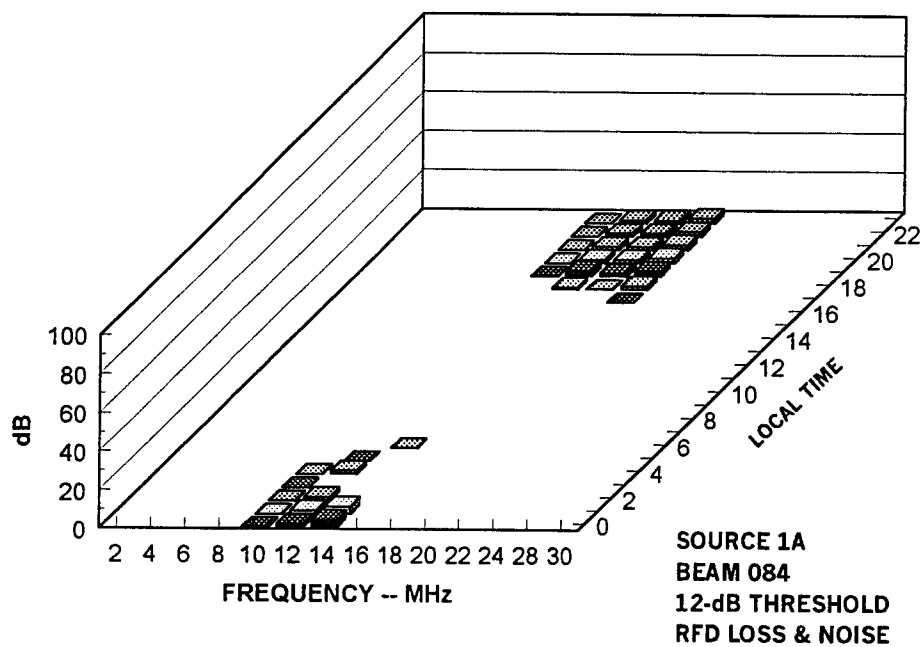


Figure 3.3-4A

Compressed View of Figure 3.3-4

Next, the impact of man-made radio noise and radio interference on signal reception was explored. Measured values of radio noise in Beam 084 (see Table 2.2.3-1) were introduced into the evaluation process. Figure 3.3-5 shows signals exceeding RFD loss and radio noise. The companion compressed view is not shown since the remaining time-frequency blocks can be counted in the primary view. RFD noise was small compared to most values of man-made noise; hence, it was ignored in this particular evaluation.

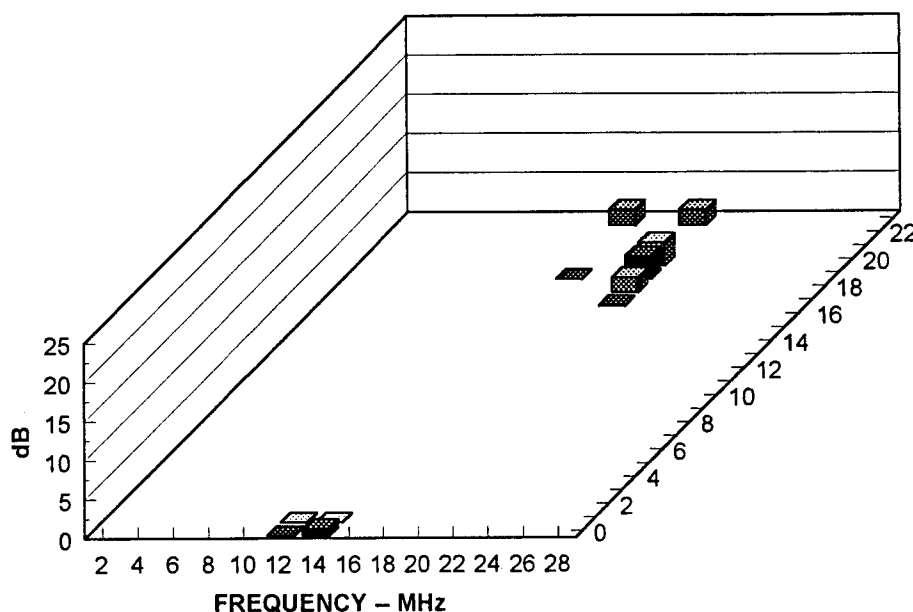


Figure 3.3-5
Signals from Source 1A Exceeding Detection Margin, RFD Loss, and
Man-made Radio Noise

Only 11 time-frequency blocks remained after all site and noise parameters were considered. Eighty-eight percent of the time-frequency bins were lost due to the combined effects of RFD loss, power-line noise, motor-controller noise, noise from two UPS, and noise from a diesel-generator-control system. This loss can be recovered by eliminating RFD loss and the sources of man-made radio noise.

3.4 RECEPTION OF SOURCE 2

Figure 3.4-1 shows the location and propagation path for Source 2. The source is located south and slightly east of the site in Beam 156. It is 2,601 kilometers from the Northwest site, and the source is within the primary coverage area of the Northwest site. Again, a transmitter power of 100 watts was used along with a typical type of mobile antenna.

Table 3.4-1 provides the field strength output of PROPHET for Source 2. The numbers indicate signal level in dB μ V at the output of the beamformer for Beam 156 and assumes there is no signal loss between the antenna elements and the beamformer output.

PET-2 reformats the PROPHET data in terms of decibels above the noise floor of the primary multicouplers for Beam 156. Any signal intercepted by the antenna elements forming Beam 156 which exceeds the multicoupler noise level is shown in the PROPHET output.

Figure 3.4-2 shows the PET-2 output for Source 2 for the time of the survey at Northwest. The data in this figure also represents Morse code signals that can be received by a manual operator who is capable of detecting such signals with a 0-dB detection threshold. This is about the capability of a well-trained Morse operator. The information in this figure is typical of the Morse signal-collection capability of the site when it was placed into operation.

Source 2 generates signals at levels above the noise floor of the primary multicouplers in 121 of the available time-frequency bins. The available frequency range is quite broad during the evening and nighttime hours, and it narrows during the daytime when absorption in the ionosphere prevents the propagation of signals at the low frequency end of the HF band. The normal diurnal changes in the range of propagating frequencies is shown in Figure 3.4-2. The data apply to the month and year of the survey at Northwest (May 1997). It will change somewhat with season and also with the 11-year sunspot cycle. The data can be rerun for any time desired to obtain updated information.

Figure 3.4-2A provides a compressed view of the data in the previous figure. This figure allows one to count the number of time-frequency bins providing useful signals from Source 2.

Distance = 2,601 kilometers Bearing = 156.3 degrees

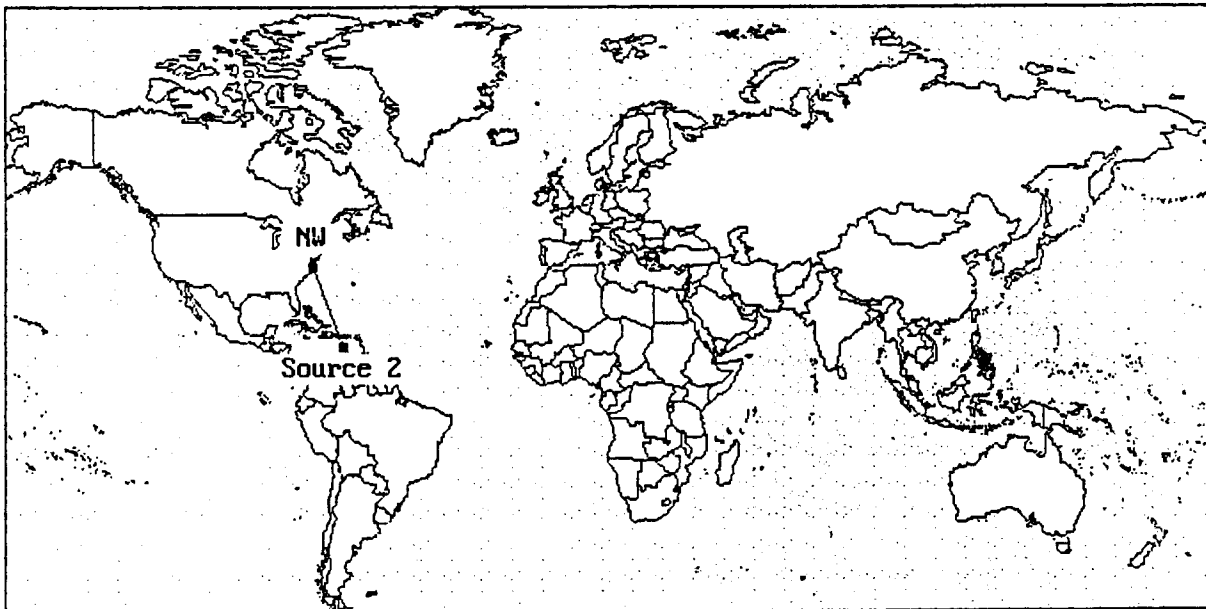


Figure 3.4-1
Map Showing the Location of Source 2

Table 3.4-1
PROPHET Output for Source 2

*** UNCLASSIFIED ***

DATE: 5/15/97 ATMOSPHERIC NOISE: NO
10.7 CM FLUX: 73.0 X-RAY FLUX: .0010 MAN-MADE NOISE: QM
SITE2 LAT: 15.0 W LON: 67.0 ANT: 111 @ *OMNI* PWR: 100.00
NW LAT: 36.5 W LON: 76.3 ANT: 115 @ *OMNI* RANGE: 2561 KM

SIGNAL STRENGTH (DB ABOVE 1 MICROVOLT)

	FREQUENCY													
TIME	2	8				16				24	32	40	LF	MF
00	-16	-9	-5	-3	-2	0	1	-10					2	17
01	-16	-9	-5	-3	-2	0	1	-7					2	18
02	-16	-9	-5	-3	-2	0	-12						2	15
03	-16	-9	-5	-3	-2	0	-20						2	15
04	-16	-9	-5	-3	-2	0							2	14
05	-16	-9	-5	-3	-2	-6							2	14
06	-16	-9	-5	-3	-2	-14							2	13
07	-16	-9	-5	-3	-2								2	12
08	-16	-9	-5	-3									2	10
09	-16	-9	-5	-3	-19								2	11
10		-15	-8	-5	-11								2	12
11		-15	-9	-6	-17								3	13

FS>

*** UNCLASSIFIED ***

DATE: 5/15/97 ATMOSPHERIC NOISE: NO
10.7 CM FLUX: 73.0 X-RAY FLUX: .0010 MAN-MADE NOISE: QM
SITE2 LAT: 15.0 W LON: 67.0 ANT: 111 @ *OMNI* PWR: 100.00
NW LAT: 36.5 W LON: 76.3 ANT: 115 @ *OMNI* RANGE: 2561 KM

SIGNAL STRENGTH (DB ABOVE 1 MICROVOLT)

	FREQUENCY													
TIME	2	8				16				24	32	40	LF	MF
12		-20	-15	-11	-6								4	14
13		-18	-14	-10	-15								5	16
14		-17	-12	-9									6	16
15		-19	-14	-10									6	17
16		-20	-15	-11	-17								6	18
17		-20	-15	-11	-12								6	18
18		-19	-14	-11	-8								6	18
19		-18	-13	-10	-6								6	18
20		-20	-15	-11	-8	-4							5	18
21		-16	-12	-7	-4	-2							5	18
22		-17	-12	-7	-4	-2	0						4	18
23		-17	-10	-6	-4	-2	0	-5					2	18

FS>

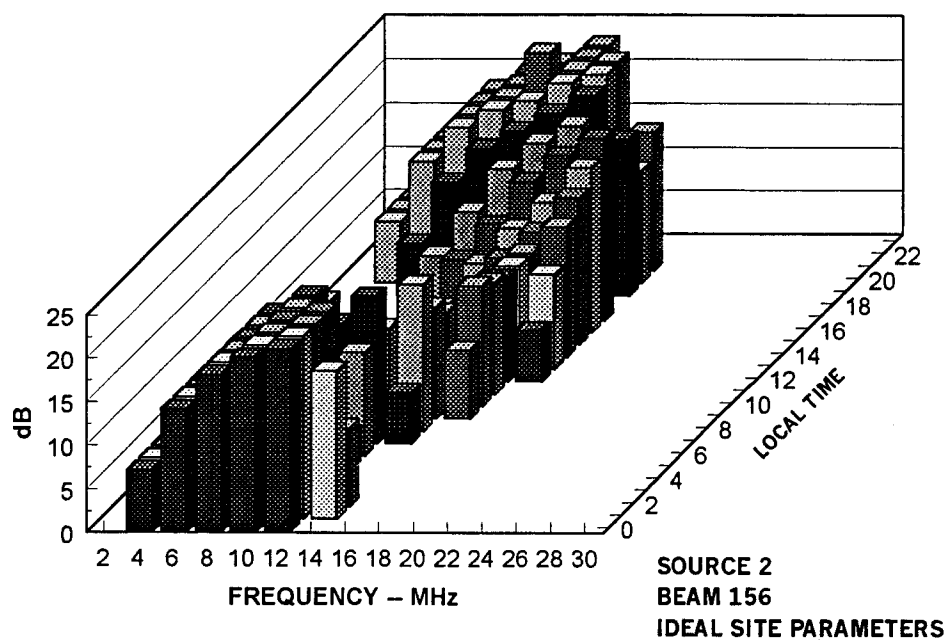


Figure 3.4-2

Signals from Source 2 Exceeding the Noise Floor of the Primary Multicouplers

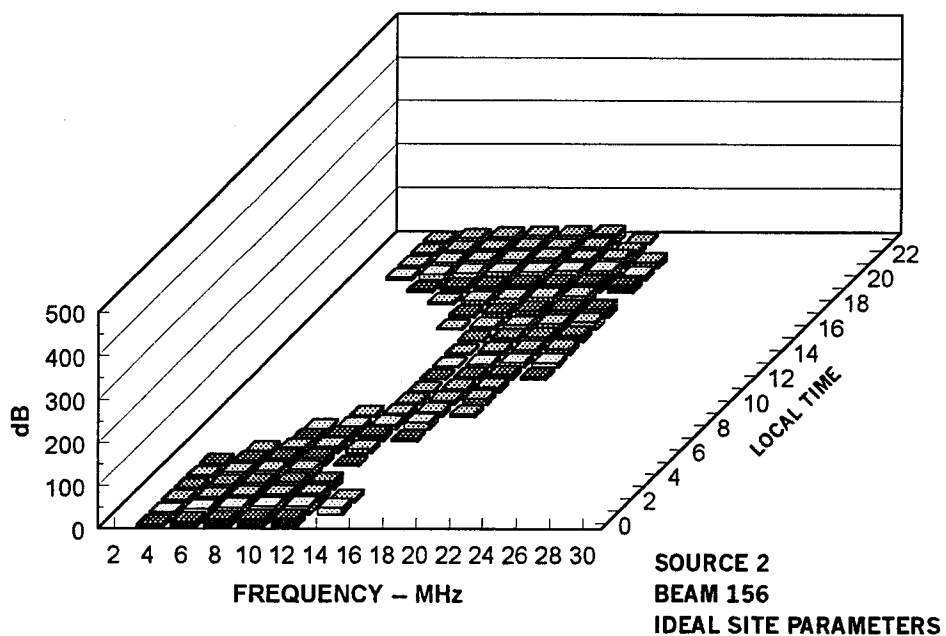


Figure 3.4-2A

Compressed View of Figure 3.4-2

The detection threshold is added to the signal-reception evaluation process. Figures 3.4-3 and 3.4-3A show signals that exceed the threshold detection level of 12 dB. Seventy-eight time-frequency bins provide detectable signals from Source 2. The amplitude scale of Figure 3.4-3 is the same as that used for the previous figure, allowing one to compare the levels of signals that exceed the prescribed detection margins (0 dB and 20 dB) for Figures 3.4-2 and 3.4-3. Any signal that exceeds the detection margin is considered to be useful, and the amount above a detection margin is somewhat academic.

Next, the impact of RFD loss and RFD noise is examined. Figures 3.4-4 and 3.4-4A show signals that exceed the combined effects of the detection margin, RFD loss, and RFD noise. A total of 38 bins can receive signals from Source 2. Forty bins are lost due to RFD loss and RFD noise, a loss of 51% of the signal-intercept capability. This decrease in signal-reception capability can be regained by eliminating RFD loss and RFD noise. This is a site design issue that needs attention.

The added impact of man-made noise from both internal and external sources is examined next. Table 2.2.3-2 provides the values for the operating noise floor for Beam 156. Since the values of noise are higher than those for Beam 084 (used for the reception of signals from Sources 1 and 1A) the adverse impact of man-made noise will be higher. No signals survived the combined impact of the detection threshold, RFD loss, RFD noise, and man-made noise. A figure depicting this is not provided.

The elimination of man-made radio noise sources would provide the signal-reception capability shown in Figure 3.4-4. The elimination of RFD loss, RFD noise, and man-made radio noise sources would return the Northwest site to the operating state described in Figure 3.4-3.

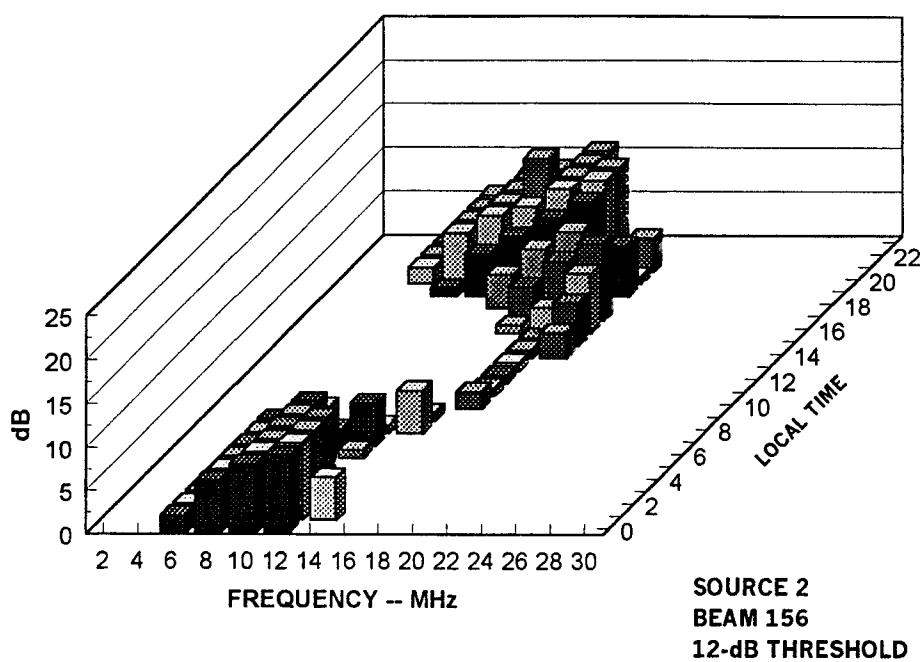


Figure 3.4-3
Signals from Source 2 Exceeding a 12-dB Threshold

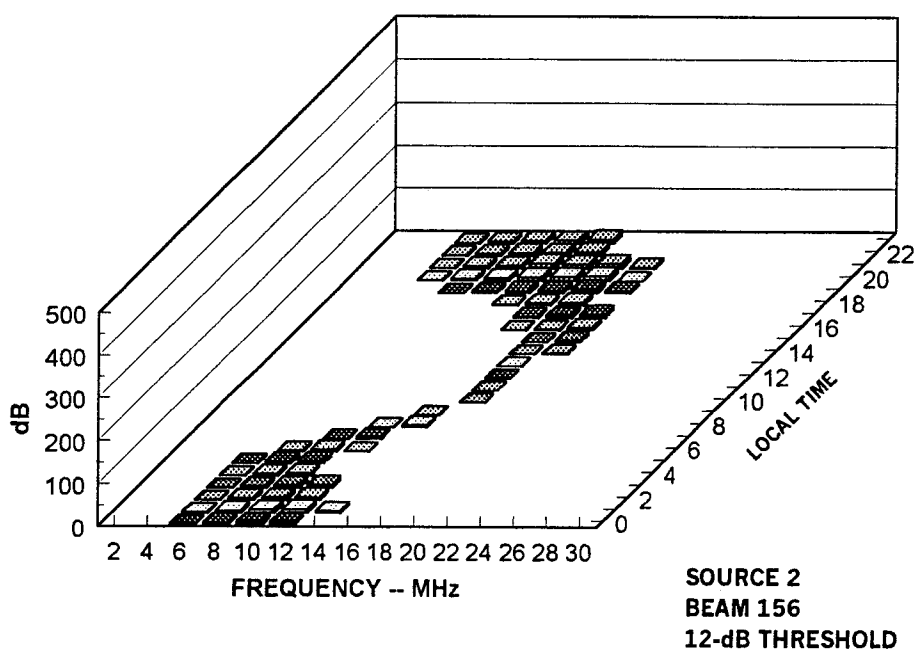


Figure 3.4-3A
Compressed View of Figure 3.4-3

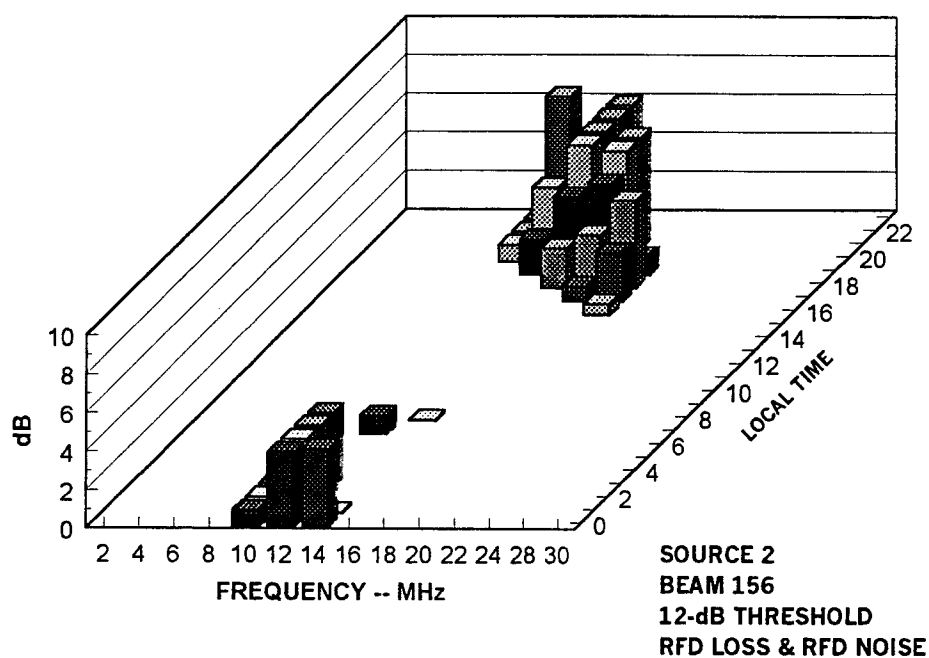


Figure 3.4-4

Signals from Source 2 Exceeding Detection Threshold, RFD Loss, and RFD Noise

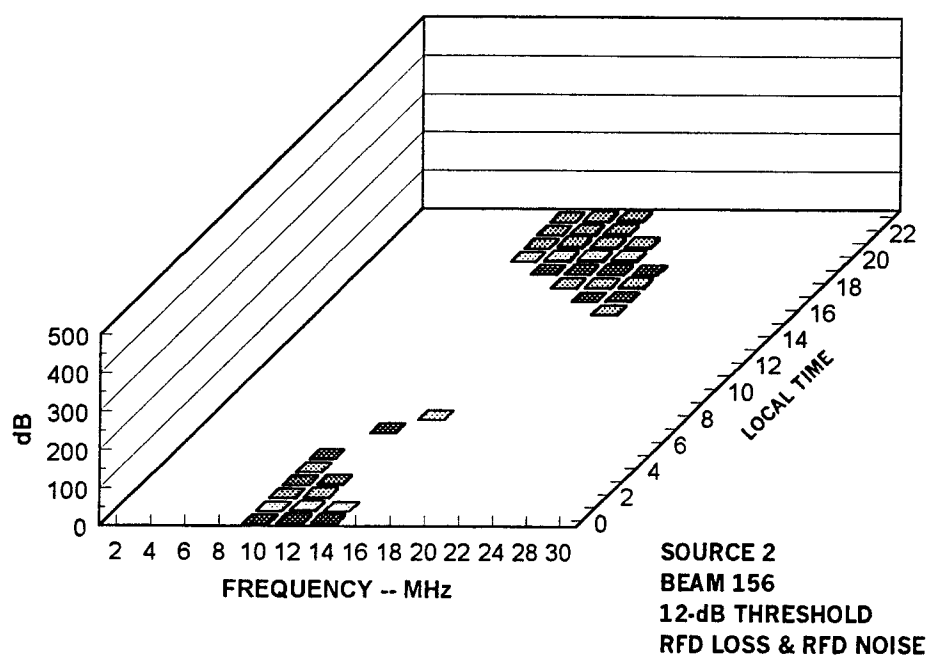


Figure 3.4-4A

Compressed View of Figure 3.4-4

3.5 RECEPTION OF SOURCE 2A

The location of Source 2A is the same as for Source 2 (see Figure 3.4-1). The transmitter power was increased from 100 to 5000 watts and the source's antenna was changed from a short whip to a full-scale conical monopole. All other site factors remained the same as for Source 2. The purpose for these changes is to investigate and illustrate the impact of source power and improved transmitter antenna parameters on signal reception.

Table 3.5-1 provides the PROPHET output for Source 2A. The signal amplitude is in dB μ V at the output of the beamformer for Beam 156. The values assume there is no signal loss between the antenna elements and the beamformer output.

The PROPHET data is reformatted by PET-2 to show received signal level above the noise floor of the primary multicouplers. Figure 3.5-1 shows the result of the reformatting. Any received signal that exceeds the noise floor is shown as a vertical bar. The height of the bar shows the amplitude of the signal above the noise floor. A significant number of signals exceed the noise floor, but not all frequency-time bins provide useful signals. The reflecting layers of the ionosphere do not support the propagation of signals from the relatively high-powered source for all the frequency and time bins provided by the HF band.

The data in Figure 3.5-1 represent signal-reception conditions from Source 2A for the month of May 1997, the time of the survey. The data in this figure provides a baseline to determine the impact of source parameters, receiving-site parameters and man-made radio noise on signal reception. It also represents the reception capability of the site to receive Morse-code signals assuming that no site or other factors degrade reception.

The number of frequency-time slots providing useful signals is somewhat larger than for the Source 2 parameters. This is because the higher transmitter power and the larger antenna at the source overcome some ionospheric absorption and allow signals to be received from additional ionospheric propagation modes. A total of 187 time-frequency blocks are provided compared with 121 for Source 2. This example shows the significant advantage obtained when monitoring high-power sources compared to the more usual low-power field-type sources of highest interest to the receiving site. The high-powered-source advantage, unless carefully understood, can result in the illusion that the site can monitor most or all signals of interest.

Figure 3.5-1A is a compressed view of the data in Figure 3.5-1.

Table 3.5-1

PROPHET Output for Source 2A

*** UNCLASSIFIED ***

DATE: 5/15/97 ATMOSPHERIC NOISE: NO
 10.7 CM FLUX: 73.0 X-RAY FLUX: .0010 MAN-MADE NOISE: QM
 SITE2A LAT: -15.0 W LON: 67.0 ANT: 181 @ *OMNI* PWR: 5000.00
 NW LAT: 36.5 W LON: 76.3 ANT: 115 @ *OMNI* RANGE: 5809 KM

SIGNAL STRENGTH (DB ABOVE 1 MICROVOLT)

TIME	FREQUENCY												LF	MF
	2	8	16	24	32	40	LF	MF						
00	-4	5	8	9	10	10	10	11	11	11	11-16	2	22	
01	-4	5	8	9	10	10	10	11	11	11	11-19	2	20	
02	-4	5	8	9	10	10	10	11	11		-9	2	19	
03	-4	5	8	9	10	10	10	11	11		-12	2	19	
04	-4	5	8	9	10	10	10	11			-4	2	17	
05	-4	5	8	9	10	10	10	11			-7	2	17	
06	-4	5	8	9	10	10	10	11			-14	2	16	
07	-4	5	8	9	10	10	10				1	2	16	
08	-4	5	8	9	10	10					-2	2	13	
09	-4	5	8	9	10	10					-12	2	13	
10	-17	1	6	8	9	9	2					2	14	
11		-11	-4	0	3	5	6-20					5	16	

FS>

*** UNCLASSIFIED ***

DATE: 5/15/97 ATMOSPHERIC NOISE: NO
 10.7 CM FLUX: 73.0 X-RAY FLUX: .0010 MAN-MADE NOISE: QM
 SITE2A LAT: -15.0 W LON: 67.0 ANT: 181 @ *OMNI* PWR: 5000.00
 NW LAT: 36.5 W LON: 76.3 ANT: 115 @ *OMNI* RANGE: 5809 KM

SIGNAL STRENGTH (DB ABOVE 1 MICROVOLT)

TIME	FREQUENCY												LF	MF
	2	8	16	24	32	40	LF	MF						
12		-16	-9	-4	-1	2	3					7	18	
13			-19	-12	-7	-4	-1	-8				8	20	
14				-20	-13	-8	-5	-2				9	21	
15					-18	-12	-8	-4	-10			9	22	
16						-20	-14	-9	-5	-3		9	22	
17							-20	-14	-10	-6	-3	9	23	
18								-19	-13	-9	-5	9	23	
19									-15	-10	-6	9	23	
20										-15	-9	8	24	
21											-12	7	23	
22												-17	6	
23													3	

FS>

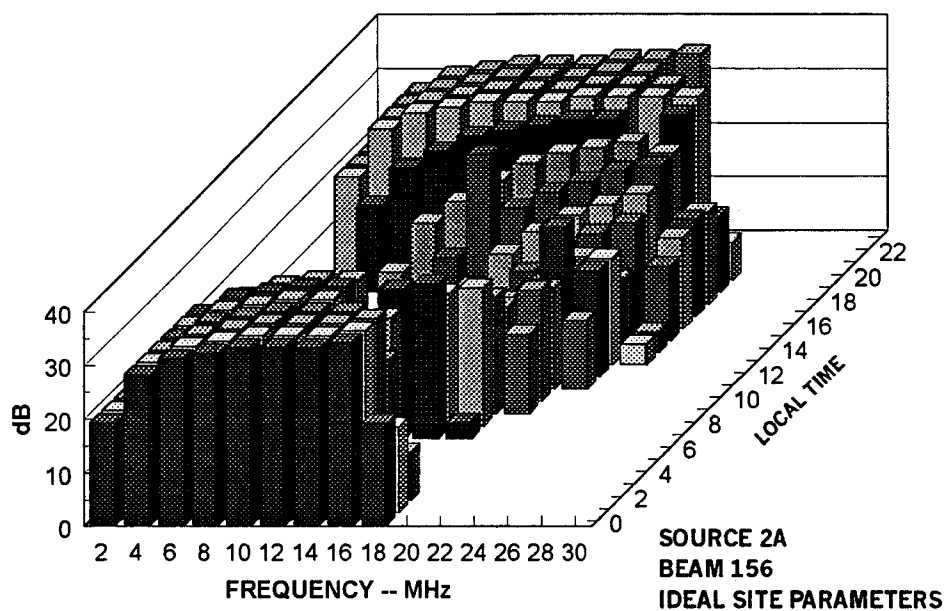


Figure 3.5-1

Signals from Source 2A Exceeding the Noise Floor of the Primary Multicouplers

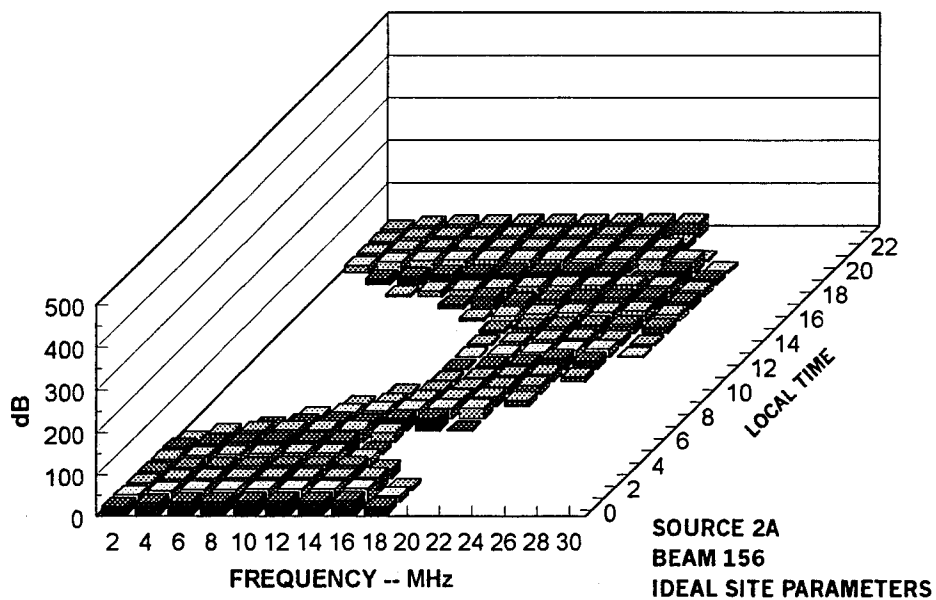


Figure 3.5-1A

Compressed View of Figure 3.5-1

The evaluation examines the machine detection of a digital signal format which requires a signal-to-noise ratio of 12 dB. Only signals more than 12-dB above the baseline of Figure 3.5-1 can be detected. Figure 3.5-2 shows the time-frequency blocks that meet this criteria. This is the modified capability that will be used to explore the signal-reception degradation from undesirable site parameters and from harmful levels of man-made radio noise. The amplitude scale of Figure 3.5-2 remains the same as for the previous example. Of interest is that any signal which exceeds the detection margin is useful. Those signals that are well above the detection threshold do not have any significant operational advantage over those that barely exceed the threshold.

Figure 3.5-2A is a compressed view of the data in Figure 3.5-2. A total of 165 time-frequency bins exceed the signal-detection threshold. Only 22 time-frequency bins are lost because of the signal-detection margin required for the automatic detection of signals from the high-power Source 2A. This is a modest penalty to pay for the automatic detection of a signal.

Figure 3.5-3 shows time-frequency bins with signals that exceed the added impact of RFD loss and RFD noise. Figure 3.5-3A is a compressed view of the data in Figure 3.5-3. One hundred and twenty-two time-frequency bins are available for the detection of the selected signal format, a loss of 43 bins. This represents a 26% loss in signal-detection capability. This loss can be regained by the elimination of RFD loss and RFD noise.

Figure 3.5-4 shows the time-frequency bins remaining after consideration of the signal-detection margin, RFD loss, RFD noise, and man-made radio noise. Figure 3.5-4A is a compressed view of the data in Figure 3.5-4. Fifty time-frequency bins survive the combined onslaught of RFD loss, RFD noise, and man-made radio noise in Beam 156. This is a loss in monitoring capability for signals from Site 2A of 70%.

While some monitoring capability remains, the decrease in capability from the combined effects of site parameters and harmful radio noise is far too high, even for a high-power source, for a well designed and operated receiving site. This loss can be completely regained by the elimination of sources of man-made radio noise (both internal and external sources), RFD loss, and RFD noise.

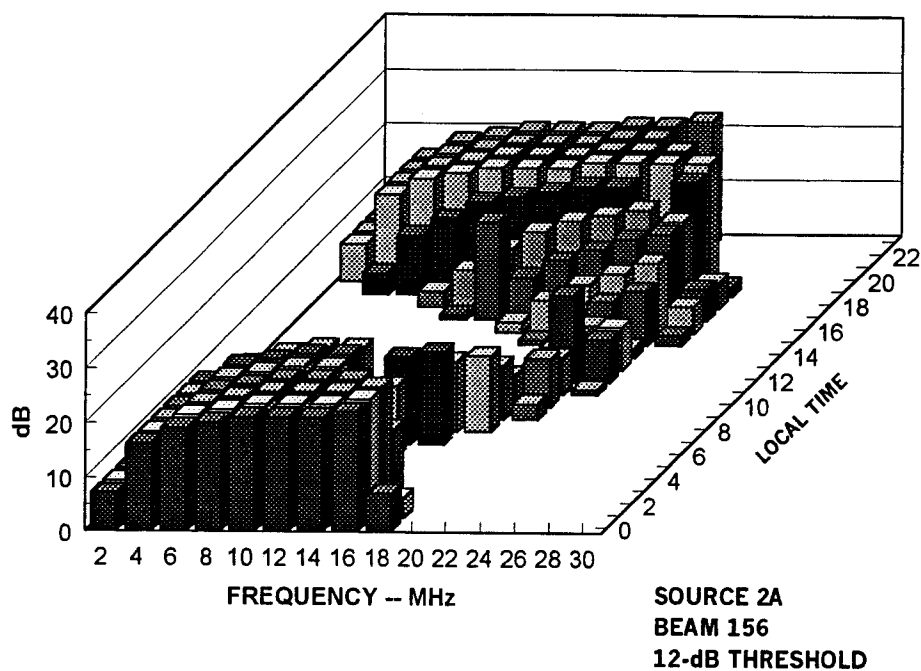


Figure 3.5-2
Signals from Source 2A Exceeding a 12-dB Threshold

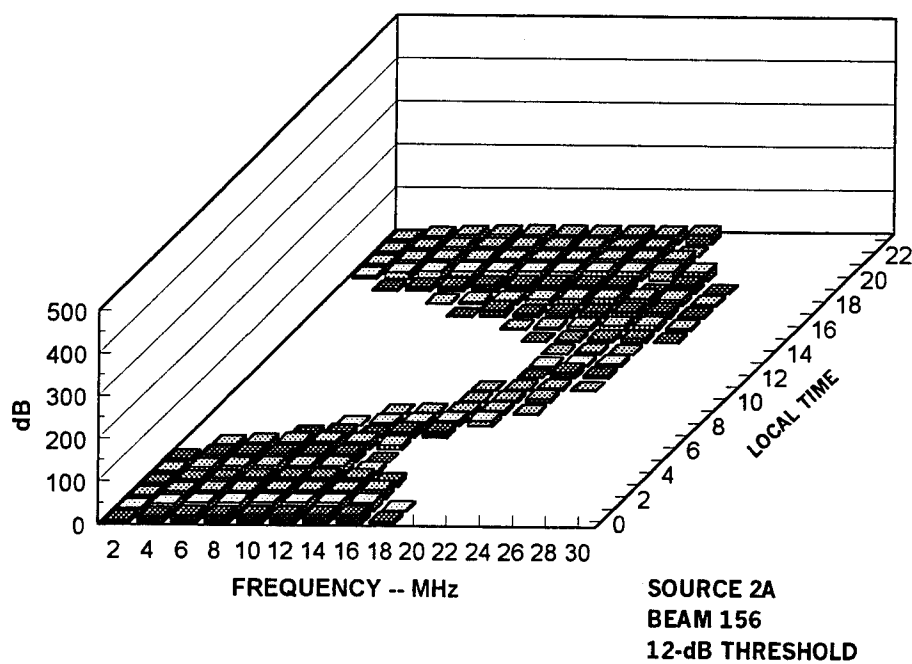


Figure 3.5-2A
Compressed View of Figure 3.5-2

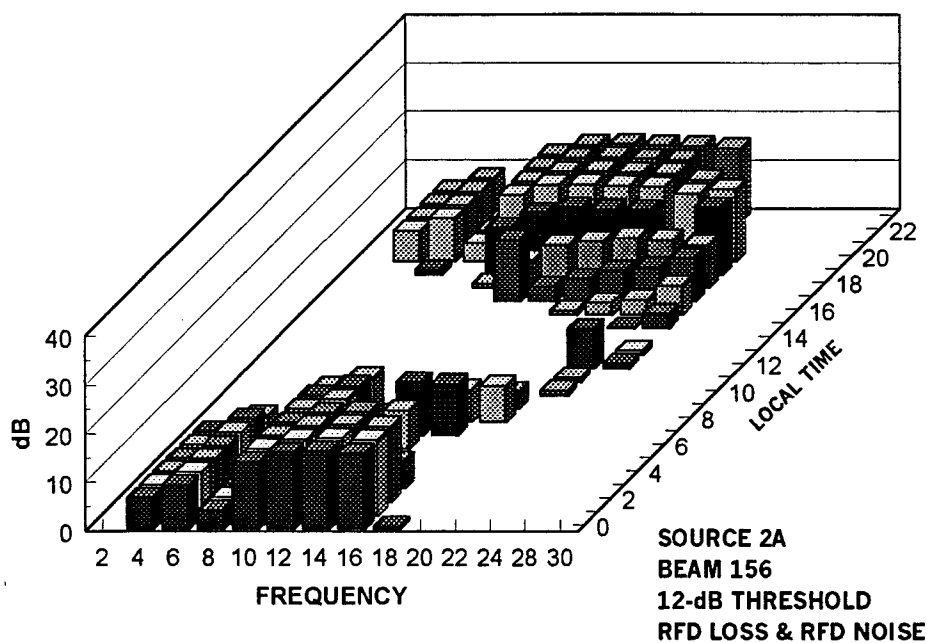


Figure 3.5-3

Signals from Source 2A Exceeding 12-dB Threshold, RFD Loss, and RFD Noise

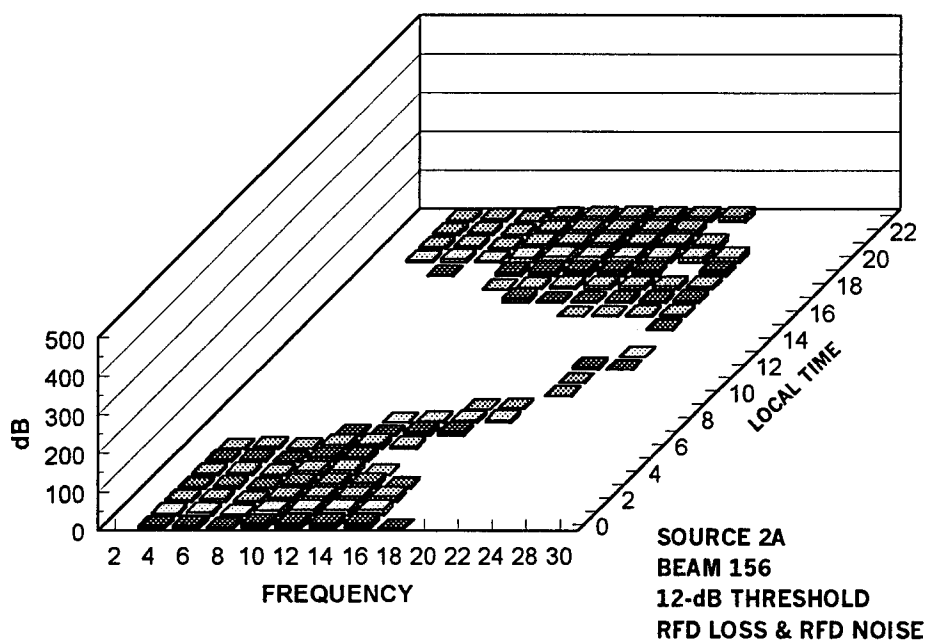


Figure 3.5-3A

Compressed View of Data in Figure 3.5-3

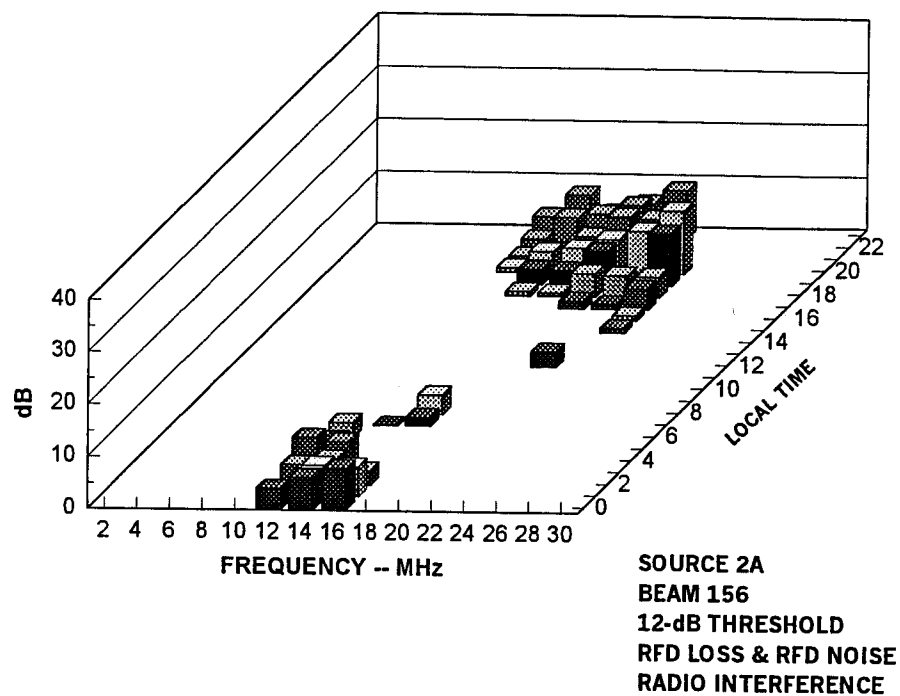


Figure 3.5-4

Signals from Source 2A Exceeding Detection Threshold, RFD Loss, and Man-Made Noise

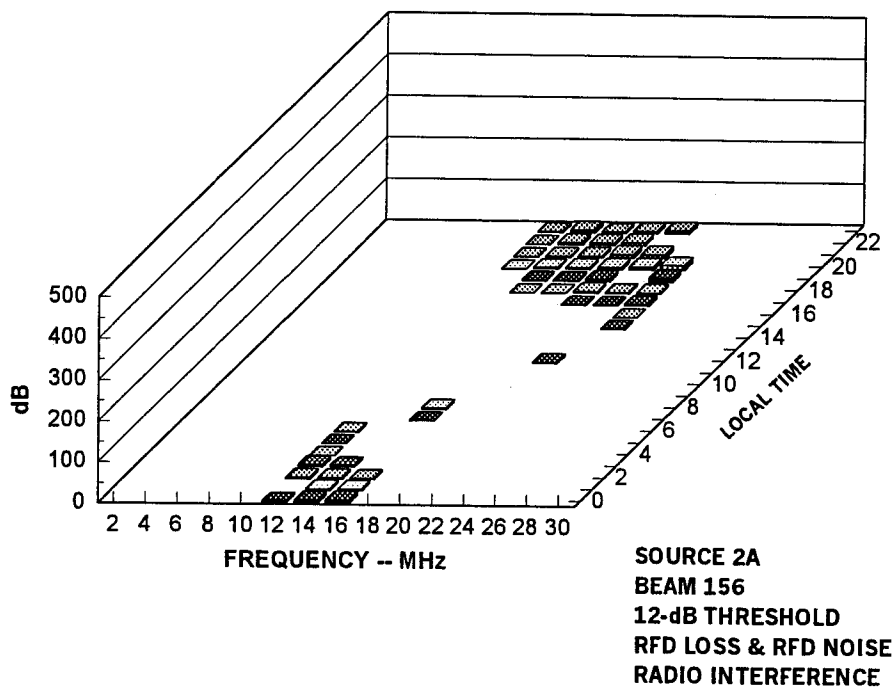


Figure 3.5-4A

Compressed View of Data in Figure 3.5-4

4. DISCUSSION

4.1 GENERAL REVIEW

The NW9705 SNEP team completed a comprehensive review of the ability of the Northwest CDAA site to receive signals of special interest. This included the identification and measurement of all significant internal and external parameters that affected the ability of the site to receive radio signals. The internal parameters consisted of signal loss between the antennas and receiving systems, the inherent noise floor of the site, the actual noise floor of the site's RFD, and the operating noise floor at the input terminals of a receiver. Sources of harmful radio interference both internal and external to the site were identified, documented, and measured. The external sources included power-line noise and interference from digital power-control devices. Quantified values of each of these factors were used to evaluate their impact on the reception of radio signals. The detailed results of this evaluation are provided in Section 3.

The signal-reception evaluation in Section 3 shows that the present condition of the Northwest CDAA site renders it marginal at best for the reception of low-level radio signals, those of special and highest interest to the site. The analysis also shows that the site can receive higher-level signals with modest success. Most of the higher-level radio signals are of little or no interest, but their reception provides the illusion that the site is properly functioning.

The team is aware that the findings of this survey are of considerable concern to all parties. Consideration must be given to the neglect of several critical electrical and electromagnetic aspects of the radio-receiving site over the past two decades; the need to keep RFD signal loss and signal contamination from internal and external sources of radio interference to an absolute minimum. This is essential because the reception of low-level signals is a major purpose of the Northwest radio-receiving facility.

Each of these factors is briefly discussed in subsequent subsections. Additional detail is provided in the preceding, more technically-oriented parts of Sections 2 and 3.

4.2 POWER-LINE NOISE

Severe radio interference from power lines was identified as a major factor adversely affecting the reception of low-level radio signals at the Northwest site by a SNEP team in 1978. It was a decade later in 1988 before a second SNEP team provided comprehensive documentation of the problem. Since that time, teams from NISE East, with the assistance of personnel from Virginia Power Company, have worked on the problem with considerable success. The major sources of power-line noise have been eliminated although several lower-level sources still exist. This has significantly reduced the level of power-line noise at the input terminals of the site's receivers. At this time the power-line noise and radio interference from other sources are about equal and both remain as significant problems. It will be necessary to continue the mitigation of power-line noise along with the mitigation of interference from other sources to return the site into a good operating site.

4.3 OTHER SOURCES OF RADIO INTERFERENCE

Radio interference from digital power-control devices is a major problem at the Northwest CDAA site. Multiple sources exist; they are located inside the Operations Building and in other buildings on the Northwest base.

Radio interference from the main UPS in the Operations Building was first identified as a source of radio interference in 1988. This interference still remains in 1997. This particular UPS is scheduled for replacement in the near future with two new UPS systems. The team is concerned that no consideration has apparently been given to the interference potential of the new UPS units. They may be better or worse than the existing system. This aspect of the new UPS units needs to be resolved prior to installation.

A second UPS in a nearby COMSAT facility operated by GE Americom was identified as a source of radio interference to receiving systems at the CDAA site. The interference from this medium-sized UPS needs to be eliminated.

The finding that two UPS units already produce significant levels of radio interference to the reception of radio signals at the Northwest site is clear warning that these devices are significant sources of radio interference. They must not be purchased or installed in or near a receiving site until all radio-interference issues are resolved.

The recent installation of a variable-speed induction-motor drive in Room 191 of the Operations Building results in excessive and harmful levels of radio interference at the input terminals of receiving systems at the site. These digital power-control devices contain a clear warning that they produce radio interference, and they should not be used at or near receiving sites unless modified to eliminate radio-interference problems. Yet, this unit was procured and installed in Room 191 in spite of the clear and explicit warning provided with the device (which is mandated by federal regulations). The NW9705 SNEP team is aware that these devices provide a better way to control the speed of standard induction motors, and there are many valuable uses for the devices. They can be used in and near a radio receiving sites if purchased to be noise-free or are modified to be noise-free prior to installation and use.

The team understands that a second such device has recently been installed in another nearby building to control air flow. We believe the second system is not yet in operation. We predict that it will cause interference to receivers at the CDAA site when it is operated.

Similar devices have been identified as sources of harmful interference at other CDAA sites. One such device causing interference to a CDAA site was located 7 km from the site. Several such devices have been modified by SNEP teams to reduce their noise production to harmless levels. The modification techniques can be applied to those units at Northwest.

Variable-speed induction-motor controllers should not be purchased or installed at or near a CDAA site unless they are purchased as radio-interference-quiet devices or are modified to be radio-interference-free devices prior to installation.

The operating noise floor data strongly suggest that inter-modulation noise generated by overloaded components in the RFD exists in the nighttime hours. This is consistent with total signal power measurements made at the Northwest site several years ago. These measurements indicated that the dynamic range of several components in the RFD is insufficient to handle the total signal power collected by the antenna elements.

4.4 SITE PARAMETERS

Signal loss and radio noise in components of the RFD also reduce the site's ability to detect and receive low-level radio signals. ENLARGER produces undesirable signal loss. In addition, the rerouting of cable trays and runs resulting in longer RF cables, the use of higher-loss cables, and the relocation of receiving systems all have increased signal loss. These actions have resulted in undesired signal loss without compensation by other means. The total signal loss in the RFD is now high enough to be of serious concern. In addition to signal loss, the Northwest ENLARGER adds some radio noise to its RF paths. These two parameters significantly decrease the signal-collection capability of the site. The signal loss and added noise from the installation of ENLARGER, while highly undesirable, is similar to that for other ENLARGER-equipped sites. Other CDAA sites employing different RF switches do not have this problem. ENLARGER should be bypassed and low-loss RF cables should be used for all critical reception tasks.

While detrimental, the adverse impact of the RFD loss and RFD-generated noise must be placed in proper context. The correction of these problems will only slightly improve the site's ability to detect and receive low-level signals. Radio-interference problems also prevent the reception of low-level signals, and this equally significant item must also be addressed and corrected.